Since January 2020 Elsevier has created a COVID-19 resource centre with free information in English and Mandarin on the novel coronavirus COVID-19. The COVID-19 resource centre is hosted on Elsevier Connect, the company's public news and information website.

Available online at www.sciencedirect.com
ScienceDirect
Mathematics and Computers in Simulation 200 (2022) 1–31
MATHEMATICS AND COMPUTERS IN SIMULATION
www.elsevier.com/locate/matcom

Original articles

A co-infection model on TB - COVID-19 with optimal control and sensitivity analysis

Shraddha Ramdas Bandekar, Mini Ghosh*

Division of Mathematics, School of Advanced Sciences, Vellore Institute of Technology, Chennai, India

Received 19 November 2021; received in revised form 17 February 2022; accepted 1 April 2022
Available online 16 April 2022

Abstract

COVID-19 had been declared a public health emergency by the World Health Organization in the early 2020. Since then, this deadly virus has claimed millions of lives worldwide. Amidst its chaotic spread, several other diseases have faced negligence in terms of treatment and care, of which one such chronic disease is Tuberculosis. Due to huge rise in COVID-19 cases, there had been a drastic decrease in notification of TB cases which resulted in reversal of global TB target progress. Apart from these due to the earlier co-infections of TB with SARS and MERS-CoV viruses, the TB-COVID-19 co-infection posed a severe threat in the spread of the disease. All these factors backed to be major motivation factor in development of this model. Leading with this concern, a TB - COVID-19 co-infection model is developed in this study, considering possibility of waning immunity of both diseases. Considering different epidemiological traits, an epidemiological model with 11 compartments is developed and the co-dynamics is analysed. A detailed stability and bifurcation analysis is performed for the TB only sub-model, COVID-19 only sub-model and the complete TB - COVID-19 model. Impact of key parameters namely, infection rate, waning immunity, and face mask efficacy on disease prevalence is discussed in detail. Sensitivity analysis by means of normalized forward sensitivity index of the basic reproduction number and LHS-PRCC approach is carried to provide a thorough understanding of significance of various parameters in accelerating as well as controlling the disease spread. Optimal control analysis is presented extensively, incorporating controls related to timely and improved TB treatment, and enhanced COVID-19 tests and isolation facilities to curb the spread of these infectious diseases. The simulation results obtained from each of these analyses stress on the importance of different control measures in mitigation of the diseases and are illustrated accordingly. The study suggests that in the times of a pandemic, other disease treatment and care must not be neglected, and adequate care must be taken so that mortality due to co-infection and unavailability of timely treatment can be avoided.

Keywords: COVID-19; Tuberculosis; Co-infection; Sensitivity; Optimal control; Latin Hypercube Sampling (LHS); Partial Rank Correlation Coefficient (PRCC)

1. Introduction

Epidemiology is one of the most important branches in medical sciences which helps in providing an overall understanding of the etiology and distribution of the disease. SARS-CoV-2 is a deadly virus which first originated in China [55] in the late 2019, and has claimed millions of lives since then. This virus spreads from person to person

* Corresponding author.
E-mail addresses: shraddha.ramdas2019@vitstudent.ac.in (S.R. Bandekar), minighosh@vit.ac.in (M. Ghosh).

https://doi.org/10.1016/j.matcom.2022.04.001

when an infected person sneezes or coughs via nasal discharge or saliva droplets which land on certain surfaces, and the contacts touch eyes nose or mouth [1,23,35]. On the other hand TB is caused due to *Mycobacterium tuberculosis* and its origin dates back to 1720 [10], and it spreads when a TB patient coughs or sneezes. Doing so these bacteria remain suspended in the form of droplets in air for several hours [46]. The former spreads through direct breathing of the droplets whereas in the latter in addition to direct contact the bacteria remains suspended for several hours and if a person happen to inhale those, he or she might get infected. The studies in [14,43] state that TB infected individuals possess higher susceptibility to COVID-19 as well as risk related to death and prolonged recovery. In the course of COVID-19 pandemic, a reduction of 21% in TB care was estimated as per data received from 84 countries [52] for period between 2019 to 2020.

TB is a highly infectious disease, and though there is treatment available for it, the annual deaths reported summed up to around 1.2 million as per [24]. Various works on TB compartmental models have been studied considering possible features of the disease. The first TB model was developed in 1962 [50], in which the researchers considered a 3 compartmental model of which one class represented latent TB infected individuals using linear difference equations providing results based on TB data of India. In 1970, the authors in [51] developed a TB model with aim to minimize the cost of TB related control interventions. In due course of times several works based on classic SIR model [27] were built to analyse the dynamics of TB disease transmission, some of which are [13,18,22,38,53], in which along with study of the disease prevalence, different controls strategies are also incorporated. In the studies [16,17], the authors worked on TB model with multiple reinfection and media impact respectively. In the former work, the authors have clearly laid out results on existence of backward bifurcation suggesting reduction in the basic reproduction number much below one for eradication of TB. In the latter study media intervention is included as a control variable to reduce disease prevalence. As of COVID-19 is concerned several works based on SEIR models have been developed and a series of results on numerical simulations and data analysis have been portrayed. The studies by [7,26,33,41] have provided a detailed analysis on the COVID-19 disease dynamics considering different regions and including control measures related to face mask, testing and treatment so on to provide mitigation strategies. In [40], the effect of lockdown is studied by modification of the disease transmission rate by including the effectiveness of individuals precautionary measures, along with COVID-19 dynamics prediction for 17 of the Indian states and the country itself. The studies [39,48] revolve around the notion of awareness by means of social media advertisements, community and global campaigns in controlling the disease transmission. The studies present a detailed analysis of the model considering the awareness efficacy parameters along with numerical simulations in terms of sensitivity analysis, disease prevalence and data fitting for the case of India. The studies by [8,42] have considered limited medical facilities factors by including treatment function to bring out a well featured analysis.

COVID-19 has proved to be an obstacle in the care, detection and treatment of several diseases like malaria, dengue, and TB etc. The report by [52] stresses on the reduction in TB detection and care with more than 1.4 million people having received no medical care for TB. The authors in [9] present a brief detail on the possibilities of TB and COVID-19 co-infection, and stress on importance of remote tracking, isolation of TB patients so that risk related to deaths can be diminished. The authors in [43] performed a detailed statistical analysis considering data of Philippines, and concluded that the COVID-19 patients are at greater risk if co-infected with TB. The study also suggested greater morbidity rates and urged on prioritizing TB medical care and detection. A similar conclusion is drawn in [14], where the authors worked on data from China.

Considering the factors mentioned in literature, a TB - COVID-19 co-infection mathematical model is built in this study and the dynamics is analysed thoroughly. The face mask factor is included in the model, as the study by [21] reveals that the infection spread could be reduced to 70% if one uses a face mask effectively. A detailed explanation on the model formulation is given is Section 2. The theoretical results on the disease dynamics based on stability and bifurcation analysis of the equilibrium points is presented as well in Section 3. Sensitivity analysis is performed to identify significant parameters in disease spread and control under Section 4. In Section 5 a detailed optimal control analysis is done by including control measures related to TB treatment and counselling along with COVID-19 detection and isolation facilities. The study ends with conclusion and a brief gist of the results.

2. Mathematical model formulation

In this research study we form an epidemiological model comprising of 11 compartments, considering co-infection of two diseases namely COVID-19 and Tuberculosis. The compartments are Susceptible (S), population

exposed to TB only (E_T), population exposed to COVID-19 only (E_C), population exposed to both TB and COVID-19 (E_{TC}), only TB infected individuals (I_T), only COVID-19 infected individuals (I_C), population infected with TB and exposed to COVID-19 (I_{TE_C}), population infected with COVID-19 and exposed to TB (I_{CE_T}), population infected with both COVID-19 and TB (I_{TC}), population recovered from TB (R_T), and population recovered from COVID-19 (R_C). The parameters involved in the model have unit as day^{-1}. We consider natural birth and death in this model and based on the below assumptions we obtain the model:

1. The transmission of disease occurs when the susceptible comes in contact with infected individuals, be it COVID-19 infected, TB infected or both. We assume that with the rising COVID-19 cases and TB in the corner, the susceptible population tends to wear face mask, thereby contributing in reducing the infection rates. These forces of infections are given by λ_T and λ_C due to TB and COVID-19 respectively, in which the face mask factor is represented by parameters α_1 and α_2.
2. It is possible that the individuals exposed to TB (E_T) only and COVID-19 only (E_C) come in contact with COVID-19 infected population and TB infected population respectively, thereby getting exposed to both these diseases.
3. The exposed population (E_T), and (E_C) move to their respective infected classes (I_T), and (I_C) at rates δ_1, and δ_2 respectively.
4. Since both diseases have different incubation period, an individual exposed to both COVID-19 and TB (E_{TC}) being infectious of both diseases at same time is unlikely. Hence, we assume that these exposed individuals move to classes I_{TE_C} and I_{CE_T} at rate ζ_1 and ζ_2 respectively. The individuals in I_{TE_C} and I_{CE_T} classes move to the I_{TC} class at rates ξ_1 and ξ_2 respectively.
5. We assume that the individuals infected with TB only can come in contact with COVID-19 infected individuals, and become exposed to the latter. In this case we assume that an enhancement factor which will act as a modification parameter in transmission of infection, would contribute in increasing the infection rate, thereby the force of infection. This parameter is given by ϵ_1 of which the value is greater than or equal to 1. The same applies to the COVID-19 only infected individuals, in which case the modification parameter is given by ϵ_2.
6. Since, both these diseases have different infectious periods, the possibility of an individual recovering from both the infections at once is neglected. Hence, an individual with this co-infection can recover from one infection at a time and move to the infected class belonging to another disease at certain rates. These rates are given by η_1 and η_2.
7. The TB only and COVID-19 only infected individuals move to their respective recovered class at rates γ_1 and γ_2 respectively.
8. Having recovered from these diseases does not guarantee lifelong immunity, hence the immunity wanes, and the recovered individuals move to the susceptible class at rates σ_1 and σ_2.
9. The infected population die at respective disease induced death rates.

The schematic diagram of our proposed model is depicted in Fig. 1. The model is framed into the following system of equations:

$$\frac{dS}{dt} = \wedge + \sigma_1 R_T + \sigma_2 R_C - (\lambda_T + \lambda_C + \mu)S \tag{1}$$

$$\frac{dE_T}{dt} = \lambda_T S - (\delta_1 + \lambda_C + \mu)E_T \tag{2}$$

$$\frac{dE_C}{dt} = \lambda_C S - (\delta_2 + \lambda_T + \mu)E_C \tag{3}$$

$$\frac{dE_{TC}}{dt} = \lambda_C E_T + \lambda_T E_C - (\zeta_1 + \zeta_2 + \mu)E_{TC} \tag{4}$$

$$\frac{dI_T}{dt} = \delta_1 E_T + \eta_1 I_{TC} - (\gamma_1 + \epsilon_1\lambda_C + \mu_1 + \mu)I_T \tag{5}$$

$$\frac{dI_C}{dt} = \delta_2 E_C + \eta_2 I_{TC} - (\gamma_2 + \epsilon_2\lambda_T + \mu_2 + \mu)I_C \tag{6}$$

$$\frac{dI_{TE_C}}{dt} = \epsilon_1\lambda_C I_T + \zeta_1 E_{TC} - (\xi_1 + \mu_3 + \mu)I_{TE_C} \tag{7}$$

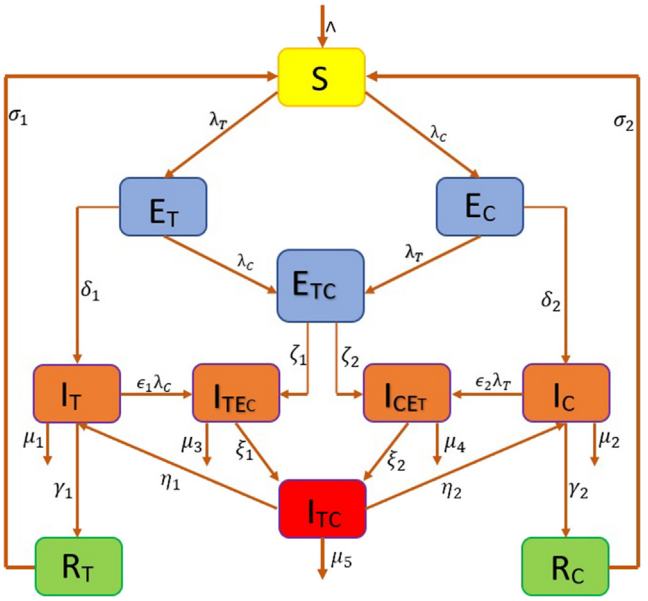

Fig. 1. Schematic diagram of the model.

$$\frac{dI_{CE_T}}{dt} = \epsilon_2\lambda_T I_C + \zeta_2 E_{TC} - (\xi_2 + \mu_4 + \mu)I_{CE_T} \tag{8}$$

$$\frac{dI_{TC}}{dt} = \xi_1 I_{TE_C} + \xi_2 I_{CE_T} - (\eta_1 + \eta_2 + +\mu_5 + \mu)I_{TC} \tag{9}$$

$$\frac{dR_T}{dt} = \gamma_1 I_T - (\sigma_1 + \mu)R_T \tag{10}$$

$$\frac{dR_C}{dt} = \gamma_2 I_C - (\sigma_2 + \mu)R_C, \tag{11}$$

where

$$\lambda_T = \beta_1(1-\alpha_1)(I_T + I_{TC} + I_{TE_C}) \text{ and } \lambda_C = \beta_2(1-\alpha_2)(I_C + I_{TC} + I_{CE_T})$$

3. Analysis of the model

3.1. TB only sub-model

The TB model is obtained by setting the following variables $E_C = E_{TC} = I_C = I_{TE_C} = I_{CE_T} = I_{TC} = R_C = 0$.

$$\begin{aligned}
\frac{dS}{dt} &= \wedge + \sigma_1 R_T - \beta_1(1-\alpha_1)I_T S - \mu S \\
\frac{dE_T}{dt} &= \beta_1(1-\alpha_1)I_T S - (\delta_1 + \mu)E_T \\
\frac{dI_T}{dt} &= \delta_1 E_T - (\gamma_1 + \mu_1 + \mu)I_T \\
\frac{dR_T}{dt} &= \gamma_1 I_T - (\sigma_1 + \mu)R_T
\end{aligned} \tag{12}$$

The total population from the model (12) is $N = S + E_T + I_T + R_T$ and hence we have $\frac{dN}{dt} = \wedge - \mu N - \mu_1 I_T$. Solving this we get $\limsup_{t\to\infty} N \leq \frac{\wedge}{\mu}$, which further implies the solution of model (12) is bounded by $\frac{\wedge}{\mu}$. Therefore, biologically feasible region for the system (12) is given by: $\Omega_T = \left\{(S, E_T, I_T, R_T) \in \mathbb{R}^4_+ : 0 \leq S, E_T, I_T, R_T \leq \frac{\wedge}{\mu}\right\}$.

3.1.1. Equilibria and basic reproduction number

The disease-free equilibrium (DFE) of the system (12) is given by $E^{0t} = \left(\frac{\wedge}{\mu}, 0, 0, 0\right)$. Using Next Generation Matrix Method [20,25,49] we find the basic reproduction number R_{0_T}.

$$\mathcal{F} = \begin{pmatrix} \beta_1(1-\alpha_1)I_T S \\ 0 \end{pmatrix} \quad \mathcal{V} = \begin{pmatrix} (\delta_1+\mu)E_T \\ -\delta_1 E_T + (\gamma_1+\mu_1+\mu)I_T \end{pmatrix}$$

The Jacobian of $\mathcal{F}$ (representing new infection terms) and $\mathcal{V}$ (representing transition terms) are F and V respectively.

$$F = \begin{pmatrix} 0 & \beta_1(1-\alpha_1)\frac{\wedge}{\mu} \\ 0 & 0 \end{pmatrix} \quad V = \begin{pmatrix} \delta_1+\mu & 0 \\ -\delta_1 & \gamma_1+\mu_1+\mu \end{pmatrix}.$$

We then obtain

$$FV^{-1} = \begin{pmatrix} \frac{\beta_1(1-\alpha_1)\delta_1\wedge}{(\delta_1+\mu)(\gamma_1+\mu_1+\mu)\mu} & \frac{\beta_1(1-\alpha_1)\wedge}{(\gamma_1+\mu_1+\mu)\mu} \\ 0 & 0 \end{pmatrix}$$

from which we obtain the basic reproduction number which is the spectral radius of FV^{-1}, given by

$$R_{0_T} = \frac{\beta_1(1-\alpha_1)\delta_1\wedge}{(\delta_1+\mu)(\gamma_1+\mu_1+\mu)\mu}$$

Theorem 3.1. *The disease-free Equilibrium given by E^{0t} is locally asymptotically stable when $R_{0_T} < 1$ and is unstable otherwise.*

Proof. The Jacobian matrix $J_{E^{0t}}$ of the system (12) at the disease-free equilibrium point E^{0t} is obtained as below:

$$J_{E^{0t}} = \begin{pmatrix} -\mu & 0 & -\beta_1(1-\alpha_1)\frac{\wedge}{\mu} & \sigma_1 \\ 0 & -(\delta_1+\mu) & \beta_1(1-\alpha_1)\frac{\wedge}{\mu} & 0 \\ 0 & \delta_1 & -(\gamma_1+\mu_1+\mu) & 0 \\ 0 & 0 & \gamma_1 & -(\sigma_1+\mu) \end{pmatrix}$$

The characteristic polynomial $|J_{E^{0t}} - \lambda I| = 0$ is given by:

$$(\lambda+\mu)\times(\lambda+(\sigma_1+\mu))\times\left(\lambda^2 + ((\delta_1+\mu)+(\gamma_1+\mu_1+\mu))\lambda + (\delta_1+\mu)(\gamma_1+\mu_1+\mu) - \beta_1(1-\alpha_1)\delta_1\frac{\wedge}{\mu}\right) = 0$$

Therefore, the eigenvalues are $-\mu < 0$, $-(\sigma_1+\mu) < 0$, and remaining are the roots of the following

$$\left(\lambda^2 + ((\delta_1+\mu)+(\gamma_1+\mu_1+\mu))\lambda + (\delta_1+\mu)(\gamma_1+\mu_1+\mu) - \beta_1(1-\alpha_1)\delta_1\frac{\wedge}{\mu}\right) = 0.$$

Hence, the two roots are:

$$-\frac{1}{2}((\delta_1+\mu)+(\gamma_1+\mu_1+\mu)) \pm \frac{1}{2}\sqrt{((\delta_1+\mu)+(\gamma_1+\mu_1+\mu))^2 - 4\left((\delta_1+\mu)(\gamma_1+\mu_1+\mu) - \beta_1(1-\alpha_1)\delta_1\frac{\wedge}{\mu}\right)}$$

which are both negative or have negative real part when $R_{0_T} < 1$ since,

$$R_{0_T} < 1 \implies (\delta_1+\mu)(\gamma_1+\mu_1+\mu) - \beta_1(1-\alpha_1)\delta_1\frac{\wedge}{\mu} > 0.$$

Therefore, the disease-free equilibrium is locally asymptotically stable when $R_{0_T} < 1$.

The endemic equilibrium $E^* = (S^*, E_T^*, I_T^*, R_T^*)$ of the system (12) is obtained to be as follows:

$$S^* = \frac{(\delta_1)(\gamma_1+\mu_1+\mu)}{\beta_1\delta_1(1-\alpha_1)}, \qquad I_T^* = \frac{(\sigma_1+\mu)(\delta_1+\mu)(\gamma_1+\mu_1+\mu)(R_{0_T}-1)}{\beta_1(1-\alpha_1)((\delta_1+\mu)(\gamma_1+\mu_1+\mu)(\sigma_1+\mu) - \sigma_1\gamma_1\delta_1)},$$

$$E_T^* = \frac{(\gamma_1+\mu_1+\mu)}{\delta_1}I_T^*, \text{ and } R_T^* = \frac{\gamma_1}{(\sigma_1+\mu)}I_T^*.$$

Clearly, the endemic equilibrium exists and is positive when $R_{0_T} > 1$ and is unique for the TB only model.

3.1.2. Bifurcation and stability analysis of the endemic equilibrium

Let us denote $S = x_1$, $E_T = x_2$, $I_T = x_3$, $R_T = x_4$, so that the TB only model (12) can be written as follows:

$$\begin{aligned}
\frac{dx_1}{dt} &= f_1 = \wedge + \sigma_1 x_4 - \beta_1(1-\alpha_1)x_3 x_1 - \mu x_1 \\
\frac{dx_2}{dt} &= f_2 = \beta_1(1-\alpha_1)x_3 x_1 - (\delta_1 + \mu)x_2 \\
\frac{dx_3}{dt} &= f_3 = \delta_1 x_2 - (\gamma_1 + \mu_1 + \mu)x_3 \\
\frac{dx_4}{dt} &= f_4 = \gamma_1 x_3 - (\sigma_1 + \mu)x_4
\end{aligned} \tag{13}$$

The Jacobian of the above system (13) at the DFE E^{0t} at the chosen bifurcation parameter β_1, obtained by equating $R_{0_T} = 1$ is

$$J_{E^{0t}(\beta_1=\beta_1^*)} = \begin{pmatrix} -\mu & 0 & -\frac{(\delta_1+\mu)(\gamma_1+\mu_1+\mu)}{\delta_1} & \sigma_1 \\ 0 & -(\delta_1+\mu) & \frac{(\delta_1+\mu)(\gamma_1+\mu_1+\mu)}{\delta_1} & 0 \\ 0 & \delta_1 & -(\gamma_1+\mu_1+\mu) & 0 \\ 0 & 0 & \gamma_1 & -(\sigma_1+\mu) \end{pmatrix}$$

Here, $\beta_1^* = \frac{(\delta_1+\mu)(\gamma_1+\mu_1+\mu)\mu}{(1-\alpha_1)\wedge\delta_1}$ obtained by equating $R_{0_T} = 1$. The above linearized system with $\beta_1 = \beta_1^*$ has a zero eigenvalue. We therefore use centre manifold theory [12,13] to analyse the dynamics of the system near $\beta_1 = \beta_1^*$. We use the theorem in [13], which we have stated in the Appendix section as Theorem A.1, to show the stability of TB only endemic equilibrium point (E^*). We now obtain the left and the right eigenvectors associated to the zero eigenvalue of the Jacobian, $J_{E^{0t}(\beta_1=\beta_1^*)}$.

Using the same notation as in Theorem A.1, we denote the right eigenvector (the column matrix) as $w = [w_1, w_2, w_3, w_4]^T$, where

$$w_1 = \frac{-((\delta_1+\mu)(\gamma_1+\mu_1+\mu)(\sigma_1+\mu) - \sigma_1\gamma_1\delta_1)w_4}{\mu\gamma_1\delta_1}, \quad w_2 = \frac{(\gamma_1+\mu_1+\mu)(\sigma_1+\mu)w_4}{\delta_1\gamma_1}$$
$$w_3 = \frac{(\sigma_1+\mu)w_4}{\gamma_1}, \quad \text{and} \quad w_4 = w_4 > 0,$$

and the left eigenvector (the row matrix) associated with the zero eigenvalue as $v = [v_1, v_2, v_3, v_4]$, where $v_1 = 0 = v_4$, $v_2 = \frac{\delta_1}{\delta_1+\mu}v_3$, and $v_3 = v_3 > 0$. Continuing as per the theorem, we now compute a and b to do the bifurcation analysis by finding the non-zero partial derivatives associated with the system (13) at the disease-free equilibrium point (E^{0t}). These partial derivatives are:

$$\frac{\partial^2 f_2}{\partial x_1 \partial x_3} = \beta_1^*(1-\alpha_1) = \frac{(\delta_1+\mu)(\gamma_1+\mu_1+\mu)\mu}{\wedge\delta_1} = \frac{\partial^2 f_2}{\partial x_3 \partial x_1}, \quad \frac{\partial^2 f_2}{\partial x_3 \partial \beta_1} = (1-\alpha_1)\frac{\wedge}{\mu}$$
$$\therefore a = -\frac{2v_3 w_4^2((\gamma_1+\mu_1+\mu)(\delta_1+\mu)(\sigma_1+\mu) - \gamma_1\delta_1\sigma_1)(\gamma_1+\mu_1+\mu)(\sigma_1+\mu)}{\wedge\delta_1\gamma_1^2} < 0$$
$$\text{and} \quad b = \frac{\delta_1 \wedge v_3 w_4(1-\alpha_1)(\sigma_1+\mu)}{\mu\gamma_1(\delta_1+\mu)} > 0.$$

Since $a < 0$ and $b > 0$, from the theorem in [13] (Theorem A.1), it implies that the unique TB only endemic equilibrium point (E^*) which exists when $R_{0_T} > 1$ will be locally asymptotically stable and the system will not exhibit any backward bifurcation at $R_{0_T} = 1$. Therefore we have the following theorem established.

Theorem 3.2. *The unique endemic equilibrium (E^*) of the system (12) is locally asymptotically stable when $R_{0_T} > 1$.*

3.2. COVID-19 only sub-model

The COVID-19 model is obtained by setting the following variables $E_T = E_{TC} = I_T = I_{TE_C} = I_{CE_T} = I_{TC} = R_T = 0$.

$$\begin{aligned}
\frac{dS}{dt} &= \wedge + \sigma_2 R_C - \beta_2(1-\alpha_2) I_C S - \mu S \\
\frac{dE_C}{dt} &= \beta_2(1-\alpha_2) I_C S - (\delta_2 + \mu) E_C \\
\frac{dI_C}{dt} &= \delta_2 E_C - (\gamma_2 + \mu_2 + \mu) I_C \\
\frac{dR_C}{dt} &= \gamma_2 I_C - (\sigma_2 + \mu) R_C
\end{aligned} \tag{14}$$

The total population from the model (14) is $N = S + E_C + I_C + R_C$ and hence we have $\frac{dN}{dt} = \wedge - \mu N - \mu_2 I_C$. Solving this we get $\limsup_{t\to\infty} N \leq \frac{\wedge}{\mu}$, which further implies the solution of model (14) is bounded by $\frac{\wedge}{\mu}$. Therefore, biologically feasible region for the system (14) is given by: $\Omega_C = \left\{(S, E_C, I_C, R_C) \in \mathbb{R}^4_+ : 0 \leq S, E_C, I_C, R_C \leq \frac{\wedge}{\mu}\right\}$.

3.2.1. Equilibria and basic reproduction number

The disease-free equilibrium (DFE) of the system (14) is given by $E^{0c} = \left(\frac{\wedge}{\mu}, 0, 0, 0\right)$. Using Next Generation Matrix Method [20,25,49] we find the basic reproduction number R_{0_C}.

$$\mathcal{F} = \begin{pmatrix} \beta_2(1-\alpha_2) I_C S \\ 0 \end{pmatrix} \quad \mathcal{V} = \begin{pmatrix} (\delta_2 + \mu) E_C \\ -\delta_2 E_C + (\gamma_2 + \mu_2 + \mu) I_C \end{pmatrix}$$

The Jacobian of $\mathcal{F}$ (representing new infection terms) and $\mathcal{V}$ (representing transition terms) are F and V respectively.

$$F = \begin{pmatrix} 0 & \beta_2(1-\alpha_2)\frac{\wedge}{\mu} \\ 0 & 0 \end{pmatrix} \quad V = \begin{pmatrix} \delta_2 + \mu & 0 \\ -\delta_2 & \gamma_2 + \mu_2 + \mu \end{pmatrix}$$

We then obtain,

$$FV^{-1} = \begin{pmatrix} \frac{\beta_2(1-\alpha_2)\delta_2 \wedge}{(\delta_2+\mu)(\gamma_2+\mu_2+\mu)\mu} & \frac{\beta_2(1-\alpha_2)\wedge}{(\gamma_2+\mu_2+\mu)\mu} \\ 0 & 0 \end{pmatrix}$$

The basic reproduction number is the spectral radius of FV^{-1}, which is given by

$$R_{0_C} = \frac{\beta_2(1-\alpha_2)\delta_2 \wedge}{(\delta_2+\mu)(\gamma_2+\mu_2+\mu)\mu}$$

Theorem 3.3. *The disease-free Equilibrium given by E^{0c} is locally asymptotically stable when $R_{0_C} < 1$ and is unstable otherwise.*

Proof. The Jacobian matrix $J_{E^{0c}}$ of the system (14) at the disease-free equilibrium point E^{0c} is obtained as below:

$$J_{E^{0c}} = \begin{pmatrix} -\mu & 0 & -\beta_2(1-\alpha_2)\frac{\wedge}{\mu} & \sigma_2 \\ 0 & -(\delta_2+\mu) & \beta_2(1-\alpha_2)\frac{\wedge}{\mu} & 0 \\ 0 & \delta_2 & -(\gamma_2+\mu_2+\mu) & 0 \\ 0 & 0 & \gamma_2 & -(\sigma_2+\mu) \end{pmatrix}$$

The characteristic polynomial $|J_{E^{0c}} - \lambda I| = 0$ is given by:

$$(\lambda+\mu)\times(\lambda+(\sigma_2+\mu))\times\left(\lambda^2 + ((\delta_2+\mu)+(\gamma_2+\mu_2+\mu))\lambda + (\delta_2+\mu)(\gamma_2+\mu_2+\mu) - \beta_2(1-\alpha_2)\delta_2\frac{\wedge}{\mu}\right) = 0$$

Therefore, the eigenvalues are $-\mu < 0$, $-(\sigma_2+\mu) < 0$, and remaining are the roots of the following

$$\left(\lambda^2 + ((\delta_2+\mu)+(\gamma_2+\mu_2+\mu))\lambda + (\delta_2+\mu)(\gamma_2+\mu_2+\mu) - \beta_2(1-\alpha_2)\delta_2\frac{\wedge}{\mu}\right) = 0.$$

Hence the two roots are:

$$-\frac{1}{2}((\delta_2+\mu)+(\gamma_2+\mu_2+\mu))\pm\frac{1}{2}\sqrt{((\delta_2+\mu)+(\gamma_2+\mu_2+\mu))^2-4\left((\delta_2+\mu)(\gamma_2+\mu_2+\mu)-\beta_2(1-\alpha_2)\delta_2\frac{\wedge}{\mu}\right)}$$

which are both negative or have negative real part when $R_{0_C}<1$ since,

$$R_{0_C}<1 \implies (\delta_2+\mu)(\gamma_2+\mu_2+\mu)-\beta_2(1-\alpha_2)\delta_2\frac{\wedge}{\mu}>0$$

Therefore, the disease-free equilibrium is locally asymptotically stable when $R_{0_C}<1$.

The endemic equilibrium $E^\star=(S^\star, E_C^\star, I_C^\star, R_C^\star)$ of the system (14) is obtained to be as follows:

$$S^\star=\frac{(\delta_2)(\gamma_2+\mu_2+\mu)}{\beta_2\delta_2(1-\alpha_2)},\ I_C^\star=\frac{(\sigma_2+\mu)(\delta_2+\mu)(\gamma_2+\mu_2+\mu)(R_{0_C}-1)}{\beta_2(1-\alpha_2)((\delta_2+\mu)(\gamma_2+\mu_2+\mu)(\sigma_2+\mu)-\sigma_2\gamma_2\delta_2)},$$

$$E_C^\star=\frac{(\gamma_2+\mu_2+\mu)}{\delta_2}I_C^\star,\ \text{and}\ R_C^\star=\frac{\gamma_2}{(\sigma_2+\mu)}I_C^\star.$$

Clearly, the COVID-19 only endemic equilibrium ($E^\star$) exists when $R_{0_C}>1$ and is unique for the COVID-19 only model (14).

3.2.2. Bifurcation and stability analysis of the endemic equilibrium

Let us denote $S=x_1,\quad E_C=x_2,\quad I_C=x_3,\quad R_C=x_4$, so that the COVID-19 only model can be written as follows:

$$\begin{aligned}
\tfrac{dx_1}{dt} &= f_1 = \wedge+\sigma_2x_4-\beta_2(1-\alpha_2)x_3x_1-\mu x_1\\
\tfrac{dx_2}{dt} &= f_2 = \beta_2(1-\alpha_2)x_3x_1-(\delta_2+\mu)x_2\\
\tfrac{dx_3}{dt} &= f_3 = \delta_2x_2-(\gamma_2+\mu_2+\mu)x_3\\
\tfrac{dx_4}{dt} &= f_4 = \gamma_2x_3-(\sigma_2+\mu)x_4
\end{aligned}\tag{15}$$

The Jacobian of the system (15) at the DFE (E^{0c}) at the chosen bifurcation parameter β_2, obtained by equating $R_{0_C}=1$ is

$$J_{E^{0c}(\beta_2=\beta_2^*)}=\begin{pmatrix}-\mu & 0 & -\frac{(\delta_2+\mu)(\gamma_2+\mu_2+\mu)}{\delta_2} & \sigma_2\\ 0 & -(\delta_2+\mu) & \frac{(\delta_2+\mu)(\gamma_2+\mu_2+\mu)}{\delta_2} & 0\\ 0 & \delta_2 & -(\gamma_2+\mu_2+\mu) & 0\\ 0 & 0 & \gamma_2 & -(\sigma_2+\mu)\end{pmatrix}$$

Here, $\beta_2^*=\frac{(\delta_2+\mu)(\gamma_2+\mu_2+\mu)\mu}{(1-\alpha_2)\wedge\delta_2}$ obtained by equating $R_{0_C}=1$. The above linearized system with $\beta_2=\beta_2^*$ has zero eigenvalue. We therefore use centre manifold theory [12,13] to analyse the dynamics of the system near $\beta_2=\beta_2^*$. We use the theorem in [13], which we have stated in the Appendix section as Theorem A.1, to show the stability of COVID-19 only endemic equilibrium point ($E^\star$). We now obtain the left and the right eigenvectors associated to the zero eigenvalue of the Jacobian $J_{E^{0c}(\beta_2=\beta_2^*)}$. Using the same notation as in Theorem A.1, we denote the right eigenvector (the column matrix) as $w=[w_1, w_2, w_3, w_4]^T$, where

$$w_1=\frac{-((\delta_2+\mu)(\gamma_2+\mu_2+\mu)(\sigma_2+\mu)-\sigma_2\gamma_2\delta_2)w_4}{\mu\gamma_2\delta_2},\quad w_2=\frac{(\gamma_2+\mu_2+\mu)(\sigma_2+\mu)w_4}{\delta_2\gamma_2}$$

$$w_3=\frac{(\sigma_2+\mu)w_4}{\gamma_2},\quad \text{and}\quad w_4=w_4>0,$$

and the left eigenvector (the row matrix) associated with the zero eigenvalue as $v=[v_1, v_2, v_3, v_4]$, where $v_1=0=v_4,\quad v_2=\frac{\delta_2}{\delta_2+\mu}v_3,\quad \text{and}\quad v_3=v_3>0.$

Continuing as per the theorem, we now compute a and b to do the bifurcation analysis by finding the non-zero partial derivatives associated with the system (15) at the disease-free equilibrium point (E^{0_C}). These partial derivatives are:

$$\frac{\partial^2 f_2}{\partial x_1 \partial x_3} = \beta_2^*(1-\alpha_2) = \frac{(\delta_2+\mu)(\gamma_2+\mu_2+\mu)\mu}{\wedge\delta_2} = \frac{\partial^2 f_2}{\partial x_3 \partial x_1}, \quad \frac{\partial^2 f_2}{\partial x_3 \partial \beta_2} = (1-\alpha_2)\frac{\wedge}{\mu}.$$

$$\therefore a = -\frac{2v_3 w_4^2((\gamma_2+\mu_2+\mu)(\delta_2+\mu)(\sigma_2+\mu) - \gamma_2\delta_2\sigma_2)(\gamma_2+\mu_2+\mu)(\sigma_2+\mu)}{\wedge\delta_2\gamma_2^2} < 0$$

$$\text{and} \quad b = \frac{\delta_2 \wedge v_3 w_4(1-\alpha_2)(\sigma_2+\mu)}{\mu\gamma_2(\delta_2+\mu)} > 0.$$

Since $a < 0$ and $b > 0$, from the theorem in [13] (Theorem A.1), it implies that the unique COVID-19 only endemic equilibrium point ($E^\star$) which exists when $R_{0_C} > 1$ will be locally asymptotically stable and the system will not exhibit any backward bifurcation at $R_{0_C} = 1$. Therefore we have the following theorem established.

Theorem 3.4. *The unique endemic equilibrium ($E^\star$) of the system (14) is locally asymptotically stable when $R_{0_C} > 1$.*

3.3. TB - COVID-19 complete model

The TB - COVID-19 complete model is given by the system of Eqs. (1)–(11). The total population from the model (1)–(11) is $N = S + E_T + E_C + E_{TC} + I_T + I_C + I_{TE_C} + I_{CE_T} + I_{TC} + R_T + R_C$ and hence we have $\frac{dN}{dt} = \wedge - \mu N - \mu_1 I_T - \mu_2 I_C - \mu_3 I_{TE_C} - \mu_4 I_{CE_T} - \mu_5 I_{TC}$. Solving this we get $\limsup_{t\to\infty} N \leq \frac{\wedge}{\mu}$, which further implies the solution of model (1)–(11) is bounded by $\frac{\wedge}{\mu}$. Therefore, biologically feasible region for the system (1)–(11) is given by:

$$\Omega_{TC} = \left\{(S, E_T, E_C, E_{TC}, I_T, I_C, I_{TE_C}, I_{CE_T}, I_{TC}, R_T, R_C) \in \mathbb{R}_+^{11} \right.$$
$$\left. : 0 \leq S, E_T, E_C, E_{TC}, I_T, I_C, I_{TE_C}, I_{CE_T}, I_{TC}, R_T, R_C \leq \frac{\wedge}{\mu}\right\}.$$

Lemma 3.5. *If $S(0) \geq 0$, $E_T(0) \geq 0$, $E_C(0) \geq 0$, $E_{TC}(0) \geq 0$, $I_T(0) \geq 0$, $I_C(0) \geq 0$, $I_{TE_C}(0) \geq 0$, $I_{CE_T}(0) \geq 0$, $I_{TC}(0) \geq 0$, $R_T(0) \geq 0$, and $R_C(0) \geq 0$, then the solutions S, E_T, E_C, E_{TC}, I_T, I_C, I_{TE_C}, I_{CE_T}, I_{TC}, R_T, R_C are positive $\forall\ t > 0$.*

Proof. We prove this lemma by method of contradiction by assuming that the total population $N(t) \neq 0\ \forall\ t \geq 0$. We assume that $\exists$ a first time t_1 such that:

$S(t_1) = 0, S'(t_1) < 0, E_T(t) \geq 0, E_C(t) \geq 0, E_{TC}(t) \geq 0, I_T(t) \geq 0, I_C(t) \geq 0, I_{TE_C}(t) \geq 0,$

$I_{CE_T}(t) \geq 0, I_{TC}(t) \geq 0, R_T(t) \geq 0,$ and $R_C(t) \geq 0$ for $t \leq 0 \leq t_1$,

$\exists$ a first time $t_2$such that :

$E_T(t_2) = 0, E_T'(t_2) < 0, S(t) \geq 0, E_C(t) \geq 0, E_{TC}(t) \geq 0, I_T(t) \geq 0, I_C(t) \geq 0, I_{TE_C}(t) \geq 0,$

$I_{CE_T}(t) \geq 0, I_{TC}(t) \geq 0, R_T(t) \geq 0,$ and $R_C(t) \geq 0$ for $t \leq 0 \leq t_2$,

$\exists$ a first time $t_3$such that :

$E_C(t_3) = 0, E_C'(t_3) < 0, S(t) \geq 0, E_T(t) \geq 0, E_{TC}(t) \geq 0, I_T(t) \geq 0, I_C(t) \geq 0, I_{TE_C}(t) \geq 0,$

$I_{CE_T}(t) \geq 0, I_{TC}(t) \geq 0, R_T(t) \geq 0,$ and $R_C(t) \geq 0$ for $t \leq 0 \leq t_3$,

$\exists$ a first time $t_4$such that :

$E_{TC}(t_4) = 0, E'_{TC}(t_4) < 0, S(t) \geq 0, E_T(t) \geq 0, E_C(t) \geq 0, I_T(t) \geq 0, I_C(t) \geq 0, I_{TE_C}(t) \geq 0,$

$I_{CE_T}(t) \geq 0, I_{TC}(t) \geq 0, R_T(t) \geq 0, and R_C(t) \geq 0 \text{ for } t \leq 0 \leq t_4,$

$\exists$ a first time $t_5$such that :

$I_T(t_5) = 0, I'_T(t_5) < 0, S(t) \geq 0, E_T(t) \geq 0, E_C(t) \geq 0, E_{TC}(t) \geq 0, I_C(t) \geq 0, I_{TE_C}(t) \geq 0,$

$I_{CE_T}(t) \geq 0, I_{TC}(t) \geq 0, R_T(t) \geq 0, \text{ and } R_C(t) \geq 0 \text{ for } t \leq 0 \leq t_5,$

$\exists$ a first time $t_6$such that :

$I_C(t_6) = 0, I'_C(t_6) < 0, S(t) \geq 0, E_T(t) \geq 0, E_C(t) \geq 0, E_{TC}(t) \geq 0, I_T(t) \geq 0, I_{TE_C}(t) \geq 0,$

$I_{CE_T}(t) \geq 0, I_{TC}(t) \geq 0, R_T(t) \geq 0, \text{ and } R_C(t) \geq 0 \text{ for } t \leq 0 \leq t_6,$

$\exists$ a first time $t_7$such that :

$I_{TE_C}(t_7) = 0, I'_{TE_C}(t_7) < 0, S(t) \geq 0, E_T(t) \geq 0, E_C(t) \geq 0, E_{TC}(t) \geq 0, I_T(t) \geq 0, I_C(t) \geq 0,$

$I_{CE_T}(t) \geq 0, I_{TC}(t) \geq 0, R_T(t) \geq 0, \text{ and } R_C(t) \geq 0 \text{ for } t \leq 0 \leq t_7,$

$\exists$ a first time $t_8$such that :

$I_{CE_T}(t_8) = 0, I'_{CE_T}(t_8) < 0, S(t) \geq 0, E_T(t) \geq 0, E_C(t) \geq 0, E_{TC}(t) \geq 0, I_T(t) \geq 0, I_C(t) \geq 0,$

$I_{TE_C}(t) \geq 0, I_{TC}(t) \geq 0, R_T(t) \geq 0, \text{ and } R_C(t) \geq 0 \text{ for } t \leq 0 \leq t_8,$

$\exists$ a first time $t_9$such that :

$I_{TC}(t_9) = 0, I'_{TC}(t_9) < 0, S(t) \geq 0, E_T(t) \geq 0, E_C(t) \geq 0, E_{TC}(t) \geq 0, I_T(t) \geq 0, I_C(t) \geq 0,$

$I_{TE_C}(t) \geq 0, I_{CE_T}(t) \geq 0, R_T(t) \geq 0, \text{ and } R_C(t) \geq 0 \text{ for } t \leq 0 \leq t_9,$

$\exists$ a first time t_{10}such that :

$R_T(t_{10}) = 0, R'_T(t_{10}) < 0, S(t) \geq 0, E_T(t) \geq 0, E_C(t) \geq 0, E_{TC}(t) \geq 0, I_T(t) \geq 0, I_C(t) \geq 0,$

$I_{TE_C}(t) \geq 0, I_{CE_T}(t) \geq 0, I_{TC}(t) \geq 0, \text{ and } R_C(t) \geq 0 \text{ for } t \leq 0 \leq t_{10},$

$\exists$ a first time t_{11}such that :

$R_C(t_{11}) = 0, R'_C(t_{11}) < 0, S(t) \geq 0, E_T(t) \geq 0, E_C(t) \geq 0, E_{TC}(t) \geq 0, I_T(t) \geq 0, I_C(t) \geq 0,$

$I_{TE_C}(t) \geq 0, I_{CE_T}(t) \geq 0, I_{TC}(t) \geq 0, \text{ and } R_T(t) \geq 0 \text{ for } t \leq 0 \leq t_{11}.$

From the above equations, we verify that, $S'(t_1) = \wedge + \sigma_1 R_T(t_1) + \sigma_2 R_C(t_1) > 0$,
$E'_T(t_2) = \beta_1(1-\alpha_1)(I_T(t_2) + I_{TC}(t_2) + I_{TE_C}(t_2))S(t_2) \geq 0$ and similarly we verify that $E'_C(t_3) \geq 0$, $E'_{TC}(t_4) \geq 0$, $I'_T(t_5) \geq 0$, $I'_C(t_6) \geq 0$, $I'_{TE_C}(t_7) \geq 0$, $I'_{CE_T}(t_8) \geq 0$, $I'_{TC}(t_9) \geq 0$, $R'_T(t_{10}) \geq 0$ and $R'_C(t_{11}) \geq 0$.

Each of these are contradicting with our assumption. Therefore, we conclude that for $t \geq 0$ we have $S(t) \geq 0$, $E_T(t) \geq 0$, $E_C(t) \geq 0$, $E_{TC}(t) \geq 0$, $I_T(t) \geq 0$, $I_C(t) \geq 0$, $I_{TE_C}(t) \geq 0$, $I_{CE_T}(t) \geq 0$, $I_{TC}(t) \geq 0$, $R_T(t) \geq 0$, and $R_C(t) \geq 0$. Hence, the solutions of the system (1)–(11) remain positive $\forall\ t \geq 0$.

3.3.1. Equilibria and basic reproduction number

The TB-COVID-19 model has 4 equilibrium points namely the disease-free equilibrium $E^0 = \left(\frac{\triangle}{\mu}, 0, 0, 0, 0, 0, 0, 0, 0, 0, 0\right)$, TB only equilibrium $E^* = (S^*, E_T^*, 0, 0, I_T^*, 0, 0, 0, 0, R_T^*, 0)$, COVID-19 only equilibrium $E^\star = (S^\star, 0, E_C^\star, 0, 0, I_C^\star, 0, 0, 0, 0, R_C^\star)$ and the endemic equilibrium (coexistence of both the disease)

$E^{**} = (S^{**}, E_T^{**}, E_C^{**}, E_{TC}^{**}, I_T^{**}, I_C^{**}, I_{TE_C}^{**}, I_{CE_T}^{**}, I_{Tc}^{**}, R_T^{**}, R_C^{**})$. The coexistence endemic equilibrium is given by:

$$S^{**} = \frac{\wedge + A_1 I_T^{**} + A_2 I_C^{**}}{A_3 z_1 + A_4 z_2 + \mu},\ E_T^{**} = \frac{A_3 z_1 S^{**}}{A_4 z_2 + (\delta_1 + \mu)},\ E_C^{**} = \frac{A_4 z_2 S^{**}}{A_3 z_1 + (\delta_2 + \mu)},$$

$$E_{TC}^{**} = \frac{A_4 z_2 E_T^{**} + A_3 z_1 E_C^{**}}{\zeta_1 + \zeta_2 + \mu},\ I_{TE_C}^{**} = \frac{\epsilon_1 A_4 z_2 I_T^{**} + \zeta_1 E_{TC}^{**}}{\xi_1 + \mu_3 + \mu},\ I_{CE_T}^{**} = \frac{\epsilon_2 A_3 z_1 I_C^{**} + \zeta_2 E_{TC}^{**}}{\xi_2 + \mu_4 + \mu},$$

$$I_{TC}^{**} = \frac{\xi_1 I_{TE_C}^{**} + \xi_2 I_{CE_T}^{**}}{\eta_1 + \eta_2 + \mu_5 + \mu},\ R_T^{**} = \frac{\gamma_1 T_T^{**}}{\sigma_1 + \mu},\ R_C^{**} = \frac{\gamma_2 T_C^{**}}{\sigma_2 + \mu}.$$

The above expressions are in $z_1,\ z_2,\ I_T,$ and I_C, where $z_1 = I_T + I_{TC} + I_{TE_C}$ and $z_2 = I_C + I_{TC} + I_{CE_T}$. This implies that these variables are in terms of $I_T,\ I_C,\ I_{TE_C},$ and I_{CE_T}. Using these we get four equations as below, which when solved gives us $I_T^{**},\ I_C^{**},\ I_{TE_C}^{**},\ I_{CE_T}^{**}$ and hence we get the endemic equilibrium E^{**}. These four equations are,

$$\begin{aligned}
&\{[A_4(I_C + C_1 I_{TE_C} + (C_2+1)I_{CE_T}) + (\delta_1+\mu)][A_3(I_T + (C_1+1)I_{TE_C} + C_2 I_{CE_T})\\
&\quad + A_4(I_C + C_1 I_{TE_C} + (C_2+1)I_{CE_T}) + \mu]\} \times [I_{TE_C}(\eta_1 C_1 - \epsilon_1\beta_2(1-\alpha_2)C_1 I_T)\\
&\quad + I_{CE_T}(\eta_1 C_2 - \epsilon_1\beta_2(1-\alpha_2)(C_2+1)I_T) - \epsilon_1\beta_2(1-\alpha_2)I_T I_C - (\gamma_1+\mu_1+\mu)I_T]\\
&\quad + \delta_1 A_3[I_T + (C_1+1)I_{TE_C} + C_2 I_{CE_T}](\wedge + A_1 I_T + A_2 I_C) = 0
\end{aligned}$$

$$\begin{aligned}
&\{[A_3(I_T + (C_1+1)I_{TE_C} + C_2 I_{CE_T}) + (\delta_2+\mu)][A_3(I_T + (C_1+1)I_{TE_C} + C_2 I_{CE_T})\\
&+ A_4(I_C + C_1 I_{TE_C} + (C_2+1)I_{CE_T}) + \mu]\} \times [I_{TE_C}(\eta_2 C_1 - \epsilon_2\beta_1(1-\alpha_1)(C_1+1)I_C)\\
&+ I_{CE_T}(\eta_2 C_2 - \epsilon_2\beta_1(1-\alpha_1)C_1 I_C) - \epsilon_2\beta_1(1-\alpha_1)I_T I_C - (\gamma_2+\mu_2+\mu)I_C]\\
&+ \delta_2 A_4[I_C + C_1 I_{TE_C} + (C_2+1)I_{CE_T}](\wedge + A_1 I_T + A_2 I_C) = 0
\end{aligned}$$

$$\begin{aligned}
&[\epsilon_1\beta_2(1-\alpha_2)(I_C + C_1 I_{TE_C} + (C_2+1)I_{CE_T})I_T - (\xi_1+\mu_3+\mu)I_{TE_C}]\\
&\quad \times \{[A_3(I_T + (C_1+1)I_{TE_C} + C_2 I_{CE_T}) + A_4(I_C + C_1 I_{TE_C} + (C_2+1)I_{CE_T}) + \mu]\\
&\quad \times [A_4(I_C + C_1 I_{TE_C} + (C_2+1)I_{CE_T}) + (\delta_1+\mu)] \times [A_3(I_T + (C_1+1)I_{TE_C} + C_2 I_{CE_T})]\}\\
&\quad + (\wedge + A_1 I_T + A_2 I_C)\{[A_3(I_T + (C_1+1)I_{TE_C} + C_2 I_{CE_T}) + (\delta_2+\mu)]\\
&\quad \times [A_3(I_T + (C_1+1)I_{TE_C} + C_2 I_{CE_T})] \times [\zeta_1 G_1(I_C + C_1 I_{TE_C} + (C_2+1)I_{CE_T})]\\
&\quad + [A_4(I_C + C_1 I_{TE_C} + (C_2+1)I_{CE_T}) + (\delta_1+\mu)]\\
&\quad \times [A_4(I_C + C_1 I_{TE_C} + (C_2+1)I_{CE_T})] \times [\zeta_1 G_2(I_T + (C_1+1)I_{TE_C} + C_2 I_{CE_T})]\} = 0
\end{aligned}$$

$$\begin{aligned}
&[\epsilon_2\beta_1(1-\alpha_1)(I_T + (C_1+1)I_{TE_C} + C_2 I_{CE_T})I_C - (\xi_2+\mu_4+\mu)I_{CE_T}]\\
&\quad \times \{[A_3(I_T + (C_1+1)I_{TE_C} + C_2 I_{CE_T}) + A_4(I_C + C_1 I_{TE_C} + (C_2+1)I_{CE_T}) + \mu]\\
&\quad \times [A_4(I_C + C_1 I_{TE_C} + (C_2+1)I_{CE_T}) + (\delta_1+\mu)] \times [A_3(I_T + (C_1+1)I_{TE_C} + C_2 I_{CE_T})]\}\\
&\quad + (\wedge + A_1 I_T + A_2 I_C)\{[A_3(I_T + (C_1+1)I_{TE_C} + C_2 I_{CE_T}) + (\delta_2+\mu)]\\
&\quad \times [A_3(I_T + (C_1+1)I_{TE_C} + C_2 I_{CE_T})] \times [\zeta_2 G_1(I_C + C_1 I_{TE_C} + (C_2+1)I_{CE_T})]\\
&\quad + [A_4(I_C + C_1 I_{TE_C} + (C_2+1)I_{CE_T}) + (\delta_1+\mu)]\\
&\quad \times [A_4(I_C + C_1 I_{TE_C} + (C_2+1)I_{CE_T})] \times [\zeta_2 G_2(I_T + (C_1+1)I_{TE_C} + C_2 I_{CE_T})]\} = 0
\end{aligned}$$

where $A_1 = \frac{\gamma_1}{\sigma_1+\mu}$, $A_2 = \frac{\gamma_2}{\sigma_2+\mu}$, $A_3 = \beta_1(1-\alpha_1)$, $A_4 = \beta_2(1-\alpha_2)$, $G_1 = \frac{A_4}{\zeta_1+\zeta_2+\mu}$, $G_2 = \frac{A_3}{\zeta_1+\zeta_2+\mu}$, $C_1 = \frac{\xi_1}{\eta_1+\eta_2+\mu_5+\mu}$, $C_2 = \frac{\xi_2}{\eta_1+\eta_2+\mu_5+\mu}$, To show the existence of a unique TB - COVID-19 endemic equilibrium point we set the parameter values as follows: $\wedge = 5679$, $\beta_1 = 1.5 \times 10^{-}6$, $\beta_2 = 3.8 \times 10^{-}5$, $\alpha_1 = 0.0001$, $\alpha_2 = 0.001$, $\sigma_1 = 0.0005$, $\sigma_2 = 0.001$, $\delta_1 = 0.07$, $\delta_2 = 0.071$, $\zeta_1 = 0.01$, $\zeta_2 = 0.07$, $\eta 1 = 0.07$, $\eta_2 = 0.0714$, $\epsilon_1 = 1.5$, $\epsilon_2 = 1.1$, $\gamma_1 = 0.006$, $\gamma_2 = 0.0714$, $\xi_1 = 0.033$, $\xi_2 = 0.01$, $\mu_1 = 0.69 \times 10^{-}4$, $\mu_2 = 0.8 \times 10 - 4$, $\mu_3 = 0.7 \times 10^{-4}$, $\mu_4 = 0.9 \times 10^{-4}$, $\mu_5 = 0.9 \times 10^{-4}$, $\mu = 0.0000425$, and obtain the TB-COVID-19 endemic equilibrium point (E^{**}) numerically by using *fsolve* in MATLAB software. We get the endemic equilibrium point to be E^{**} = (250.96, 14.85, 4757.06, 19211.94, 155.51, 10023.43, 109 971.88, 336 642.98, 50 810.22, 3930.57, 430 234.93).

3.3.2. Stability analysis of the disease free equilibrium E^0

The DFE of the TB-COVID-19 model is $E^0 = \left(\frac{\wedge}{\mu}, 0, 0, 0, 0, 0, 0, 0, 0, 0, 0\right)$. We have obtained the basic reproduction numbers of the TB only sub-model and COVID-19 only sub-model in the previous sections. Using the theorem in [49], the basic reproduction number (R_0) of the TB-COVID-19 complete model is given as:

$$R_0 = \max\{R_{0_T}, R_{0_C}\}.$$

Theorem 3.6. *The disease-free Equilibrium given by E^0 is locally asymptotically stable when $R_0 < 1$ and is unstable otherwise.*

The Jacobian matrix J_{E^0} of the system (1)–(11) at the disease-free equilibrium point E^0 is obtained as below:

$$J_{E^0} = \begin{bmatrix} -\mu & 0 & 0 & 0 & -a_{15} & -a_{16} & -a_{15} & -a_{16} & -a_{17} & \sigma_1 & \sigma_2 \\ 0 & -a_{22} & 0 & 0 & a_{15} & 0 & a_{15} & 0 & a_{15} & 0 & 0 \\ 0 & 0 & -a_{33} & 0 & 0 & a_{16} & 0 & a_{16} & a_{16} & 0 & 0 \\ 0 & 0 & 0 & -a_{44} & 0 & 0 & 0 & 0 & 0 & 0 & 0 \\ 0 & \delta_1 & 0 & 0 & -a_{55} & 0 & 0 & 0 & \eta_1 & 0 & 0 \\ 0 & 0 & \delta_2 & 0 & 0 & -a_{66} & 0 & 0 & \eta_2 & 0 & 0 \\ 0 & 0 & 0 & \zeta_1 & 0 & 0 & -a_{77} & 0 & 0 & 0 & 0 \\ 0 & 0 & 0 & \zeta_2 & 0 & 0 & 0 & -a_{88} & 0 & 0 & 0 \\ 0 & 0 & 0 & 0 & 0 & 0 & \xi_1 & \xi_2 & -a_{99} & 0 & 0 \\ 0 & 0 & 0 & 0 & \gamma_1 & 0 & 0 & 0 & 0 & -(\sigma_1+\mu) & 0 \\ 0 & 0 & 0 & 0 & 0 & \gamma_2 & 0 & 0 & 0 & 0 & -(\sigma_2+\mu) \end{bmatrix},$$

where

$$a_{15} = \beta_1(1-\alpha_1)\frac{\wedge}{\mu}, \quad a_{16} = \beta_2(1-\alpha_2)\frac{\wedge}{\mu}, \quad a_{17} = (\beta_1(1-\alpha_1)+\beta_2(1-\alpha_2))\frac{\wedge}{\mu}$$
$$a_{22} = \delta_1+\mu, \quad a_{33} = \delta_2+\mu, \quad a_{44} = \zeta_1+\zeta_2+\mu, \quad a_{55} = \gamma_1+\mu_1+\mu, \quad a_{66} = \gamma_2+\mu_2+\mu$$
$$a_{77} = \xi_1+\mu_3+\mu, \quad a_{88} = \xi_2+\mu_4+\mu, \quad a_{99} = \eta_1+\eta_2+\mu_5+\mu.$$

The characteristic polynomial is given by:

$$(\lambda+a_{44})\times(\lambda+a_{77})\times(\lambda+a_{88})\times(\lambda+a_{99})\times(\lambda+(\sigma_1+\mu))\times(\lambda+(\sigma_2+\mu))\times(\lambda^2+M_1\lambda+Q_1)\times(\lambda^2+M_2\lambda+Q_2) = 0,$$

where

$$M_1 = (\delta_1+\mu)+(\gamma_1+\mu_1+\mu), \quad Q_1 = (\delta_1+\mu)(\gamma_1+\mu_1+\mu) - \beta_1(1-\alpha_1)\delta_1\frac{\wedge}{\mu}$$
$$M_2 = (\delta_2+\mu)+(\gamma_2+\mu_2+\mu), \quad Q_2 = (\delta_2+\mu)(\gamma_2+\mu_2+\mu) - \beta_2(1-\alpha_2)\delta_2\frac{\wedge}{\mu}$$

We observe that all the eigenvalues will be negative or will have negative real part when $R_0 < 1$. Since R_0 is maximum of R_{0_T} and R_{0_C}, clearly the roots of both the quadratic polynomials will be either negative or have negative real part when the basic reproduction number is lesser than 1. The explanation stands same as in previous two sections.

3.3.3. Bifurcation and stability analysis of endemic equilibrium E^{**}

Let us denote $S = x_1$, $E_T = x_2$, $E_C = x_3$, $E_{TC} = x_4$, $I_T = x_5$, $I_C = x_6$, $I_{TE_C} = x_7$, $I_{CE_T} = x_8$, $I_{TC} = x_9$, $R_T = x_{10}$, $R_C = x_{11}$, so that the TB-COVID-19 model can be written as follows:

$$\begin{aligned}
\frac{dx_1}{dt} &= f_1 = \wedge + \sigma_1 x_{10} + \sigma_2 x_{11} - (\lambda_T + \lambda_C + \mu)x_1 \\
\frac{dx_2}{dt} &= f_2 = \lambda_T x_1 - (\delta_1 + \lambda_C + \mu)x_2 \\
\frac{dx_3}{dt} &= f_3 = \lambda_C x_1 - (\delta_2 + \lambda_T + \mu)x_3 \\
\frac{dx_4}{dt} &= f_4 = \lambda_C x_2 + \lambda_T x_3 - (\zeta_1 + \zeta_2 + \mu)x_4 \\
\frac{dx_5}{dt} &= f_5 = \delta_1 x_2 + \eta_1 x_9 - (\gamma_1 + \epsilon_1\lambda_C + \mu_1 + \mu)x_5 \\
\frac{dx_6}{dt} &= f_6 = \delta_2 x_3 + \eta_2 x_9 - (\gamma_2 + \epsilon_2\lambda_T + \mu_2 + \mu)x_6 \\
\frac{dx_7}{dt} &= f_7 = \epsilon_1\lambda_C x_5 + \zeta_1 x_4 - (\xi_1 + \mu_3 + \mu)x_7 \\
\frac{dx_8}{dt} &= f_8 = \epsilon_2\lambda_T x_6 + \zeta_2 x_4 - (\xi_2 + \mu_4 + \mu)x_8 \\
\frac{dx_9}{dt} &= f_9 = \xi_1 x_7 + \xi_2 x_8 - (\eta_1 + \eta_2 + +\mu_5 + \mu)x_9 \\
\frac{dx_{10}}{dt} &= f_{10} = \gamma_1 x_5 - (\sigma_1 + \mu)x_{10} \\
\frac{dx_{11}}{dt} &= f_{11} = \gamma_2 x_6 - (\sigma_2 + \mu)x_{11},
\end{aligned} \tag{16}$$

where

$$\lambda_T = \beta_1(1-\alpha_1)(x_5 + x_9 + x_7) \text{ and } \lambda_C = \beta_2(1-\alpha_2)(x_6 + x_9 + x_8)$$

The Jacobian of the above system at the DFE E^0 at the chosen bifurcation parameter β_2, obtained by equating $R_{0_C} = 1$ is

$$J_{E^0(\beta_2=\beta_2^*)} = \begin{bmatrix}
-\mu & 0 & 0 & 0 & -a_{15} & -a_{16}^* & -a_{15} & -a_{16}^* & -a_{17}^* & \sigma_1 & \sigma_2 \\
0 & -a_{22} & 0 & 0 & a_{15} & 0 & a_{15} & 0 & a_{15} & 0 & 0 \\
0 & 0 & -a_{33} & 0 & 0 & a_{16}^* & 0 & a_{16}^* & a_{16}^* & 0 & 0 \\
0 & 0 & 0 & -a_{44} & 0 & 0 & 0 & 0 & 0 & 0 & 0 \\
0 & \delta_1 & 0 & 0 & -a_{55} & 0 & 0 & 0 & \eta_1 & 0 & 0 \\
0 & 0 & \delta_2 & 0 & 0 & -a_{66} & 0 & 0 & \eta_2 & 0 & 0 \\
0 & 0 & 0 & \zeta_1 & 0 & 0 & -a_{77} & 0 & 0 & 0 & 0 \\
0 & 0 & 0 & \zeta_2 & 0 & 0 & 0 & -a_{88} & 0 & 0 & 0 \\
0 & 0 & 0 & 0 & 0 & 0 & \xi_1 & \xi_2 & -a_{99} & 0 & 0 \\
0 & 0 & 0 & 0 & \gamma_1 & 0 & 0 & 0 & 0 & -(\sigma_1+\mu) & 0 \\
0 & 0 & 0 & 0 & 0 & \gamma_2 & 0 & 0 & 0 & 0 & -(\sigma_2+\mu)
\end{bmatrix},$$

where

$$\begin{aligned}
&a_{15} = \beta_1(1-\alpha_1)\frac{\wedge}{\mu}, \quad a_{16}^* = \beta_2^*(1-\alpha_2)\frac{\wedge}{\mu}, \quad a_{17}^* = (\beta_1(1-\alpha_1) + \beta_2^*(1-\alpha_2))\frac{\wedge}{\mu} \\
&a_{22} = \delta_1 + \mu, \quad a_{33} = \delta_2 + \mu, \quad a_{44} = \zeta_1 + \zeta_2 + \mu, \quad a_{55} = \gamma_1 + \mu_1 + \mu, \quad a_{66} = \gamma_2 + \mu_2 + \mu \\
&a_{77} = \xi_1 + \mu_3 + \mu, \quad a_{88} = \xi_2 + \mu_4 + \mu, \quad a_{99} = \eta_1 + \eta_2 + \mu_5 + \mu
\end{aligned}$$

Here, $\beta_2^* = \frac{(\delta_2+\mu)(\gamma_2+\mu_2+\mu)\mu}{(1-\alpha_2)\wedge\delta_2}$ obtained by equating $R_0 = R_{0_C} = 1$. The above linearized system with $\beta_2 = \beta_2^*$ has zero eigenvalue. We then analyse the dynamics of the system near $\beta_2 = \beta_2^*$ by using the theorem in [13] as mentioned in the previous two sections. We now obtain the left and the right eigenvectors associated to

the zero eigenvalue of the Jacobian $J_{E^0(\beta_2=\beta_2^*)}$. We denote the right eigenvector (the column matrix) as $w = [w_1, w_2, w_3, w_4, w_5, w_6, w_7, w_8, w_9, w_{10}, w_{11}]^T$, where

$$w_2 = w_4 = w_5 = w_7 = w_8 = w_9 = w_{10} = 0,$$
$$w_1 = \frac{-((\delta_2+\mu)(\gamma_2+\mu_2+\mu)(\sigma_2+\mu)-\sigma_2\gamma_2\delta_1)w_{11}}{\mu\gamma_2\delta_2}, \quad w_3 = \frac{(\gamma_2+\mu_2+\mu)(\sigma_2+\mu)w_{11}}{\delta_2\gamma_2}$$
$$w_6 = \frac{(\sigma_2+\mu)w_{11}}{\gamma_2}, \quad \text{and} \quad w_{11} = w_{11} > 0,$$

and the left eigenvector (the row matrix) associated with the zero eigenvalue as $v = [v_1, v_2, v_3, v_4, v_5, v_6, v_7, v_8, v_9, v_{10}, v_{11}]$, where

$$v_1 = v_2 = v_5 = v_{10} = v_{11} = 0$$
$$v_6 = \frac{\delta_2+\mu}{\delta_2}v_3, \quad v_9 = \frac{(\delta_2+\mu)(\gamma_2+\mu_2+\mu+\eta_2)}{\delta_2(\eta_1+\eta_2+\mu_5+\mu)}v_3, \quad v_7 = \frac{\xi_1(\delta_2+\mu)(\gamma_2+\mu_2+\mu+\eta_2)}{\delta_2(\eta_1+\eta_2+\mu_5+\mu)(\xi_1+\mu_3+\mu)}v_3$$
$$v_4 = \frac{1}{(\zeta_1+\zeta_2+\mu)}\left[\frac{\zeta_1\xi_1(\delta_2+\mu)(\gamma_2+\mu_2+\mu+\eta_2)}{\delta_2(\eta_1+\eta_2+\mu_5+\mu)(\xi_1+\mu_3+\mu)} + \frac{\zeta_2}{(\xi_2+\mu_4+\mu)}\right.$$
$$\left.\times\left(\frac{\xi_2(\delta_2+\mu)(\gamma_2+\mu_2+\mu+\eta_2)}{\delta_2(\eta_1+\eta_2+\mu_5+\mu)} + \frac{(\delta_2+\mu)(\gamma_2+\mu_2+\mu)}{\delta_2}\right)\right]v_3$$
$$v_8 = \frac{1}{(\xi_2+\mu_4+\mu)}\left(\frac{\xi_2(\delta_2+\mu)(\gamma_2+\mu_2+\mu+\eta_2)}{\delta_2(\eta_1+\eta_2+\mu_5+\mu)} + \frac{(\delta_2+\mu)(\gamma_2+\mu_2+\mu)}{\delta_2}\right)v_3, \text{ and } v_3 = v_3 > 0$$

Continuing as per the theorem in [13], we compute a and b to do the bifurcation analysis by finding the non-zero partial derivatives associated with the system (16) at the disease-free equilibrium point (E^0). These non-zero partial derivatives are :

$$\frac{\partial^2 f_3}{\partial x_1 \partial x_6} = \beta_2^*(1-\alpha_2) = \frac{(\delta_2+\mu)(\gamma_2+\mu_2+\mu)\mu}{\wedge\delta_2} = \frac{\partial^2 f_3}{\partial x_6 \partial x_1}, \quad \frac{\partial^2 f_3}{\partial x_6 \partial \beta_2} = (1-\alpha_2)\frac{\wedge}{\mu}$$
$$\therefore a = -\frac{2V_3W_{11}^2((\gamma_2+\mu_2+\mu)(\delta_2+\mu)(\sigma_2+\mu)-\gamma_2\delta_2\sigma_2)(\gamma_2+\mu_2+\mu)(\sigma_2+\mu)(\delta_2+\mu)}{\wedge\delta_2^2\gamma_2^2} < 0$$
$$\text{and} \quad b = \frac{\delta_1 \wedge V_3W_4(1-\alpha_1)(\sigma_1+\mu)}{\mu\gamma_1(\delta_1+\mu)} > 0$$

Since $a < 0$ and $b > 0$, from the theorem in [13] (Theorem A.1) it implies that the unique co-existence endemic equilibrium point (E^{**}) which exists when $R_0 = R_{0_C} > R_{0_T} > 1$ will be locally asymptotically stable and the system will not exhibit any backward bifurcation at $R_0 = 1$. Therefore we have the following theorem established.

Theorem 3.7. *The unique endemic equilibrium (E^{**}) of the system (1)–(11) is locally asymptotically stable when $R_0 = R_{0_C} > R_{0_T} > 1$.*

4. Numerical simulation

To achieve a better insight on the dynamics of the model, the illustration of the model solution and disease prevalence is provided graphically along with sensitivity analysis by means of forward sensitivity index and PRCC in this section. The values of few parameters in the model are obtained from the literature and the rest are assumed in a realistic manner to carry out the simulations. We consider the data related to India to perform the simulations, as India is one of the worst affected country due to COVID-19 as well as TB disease is prevalent in the country. As per the data from [2,3], during the period between 19 September 2020 to 2021 a total of 23.2 million COVID-19 cases were confirmed in India, and as per [4,5] total TB cases ranging between 0.4 million to 0.58 million have been reported in 2021. To set the value of β_2, we use the TB provisional data from [6,46], wherein a total of 1.6 million plus TB cases were reported in 2020 in India. The total population of India equals near 1397 million, and by applying the unit conversion we get the TB infection rate (β_1) to be 7×10^{-6} and COVID-19 infection rate (β_2) as 5×10^{-5}. The recruitment rate ($\wedge$), natural death rate (μ) are demographic and the other parameters are taken from several studies and few are realistically assumed. The remaining parameters are listed in Table 1.

Table 1
Model parameters.

Parameters	Meaning	Value	Reference
$\wedge$	Recruitment rate	5	Varies
α_1	TB Mask usage parameter	[0,1]	Varies
α_2	COVID-19 Mask usage parameter	0.05	[19,34]
σ_1	Waning rate from R_T to S	0.0005	Assumed
σ_2	Waning rate from R_C to S	0.001	Assumed
δ_1	Rate at which TB exposed become TB infectious	[0.01,0.071]	[46,47]
δ_2	Rate at which COVID-19 exposed become COVID-19 infectious	[0.071,0.33]	[29,31]
ζ_1	Progression from E_{TC} to I_{TE_C}	0.01	Assumed
ζ_2	Progression from E_{TC} to I_{CE_T}	0.07	Assumed
η_1	Rate at which co-infected individuals (I_{TC}) recover from COVID-19 only	0.0714	[44,54]
η_2	Rate at which co-infected individuals (I_{TC}) recover from TB only	[0.004,0.07]	[46,47]
ϵ_1	Factor that enhances acquiring of COVID-19 infection after being infected with TB	1.5	Assumed
ϵ_2	Factor that enhances acquiring of TB infection after being infected with COVID-19	1.1	Assumed
γ_1	Recovery rate of I_T	[0.004,0.07]	[46,47]
γ_2	Recovery rate of I_C	0.0714	[44,54]
ξ_1	Progression from I_{TE_C} to I_{TC}	0.033	Assumed
ξ_2	Progression from I_{CE_T} to I_{TC}	0.033	Assumed
μ_1	Death rate of I_T	0.69×10^{-4}	Assumed
μ_2	Death rate of I_C	0.8×10^{-4}	Assumed
μ_3	Death rate of I_{TE_C}	0.7×10^{-4}	Assumed
μ_4	Death rate of I_{CE_T}	0.9×10^{-4}	Assumed
μ_5	Death rate of I_{TC}	0.9×10^{-4}	Assumed
μ	Natural death rate	0.0000425	Demographic

The model solution is presented in Fig. 2, from which we observe the variation in each variable over a time period of 400 days. The parameter values are as in Table 1. Fig. 3 represents the variation in total infected and total recovered population with increase or decrease in the respective parameter values. In Fig. 3, we showcase the impact of simultaneous change key parameters on the total infected and recovered population. Fig. 3(a) clearly signifies importance of the face mask factor in reducing the number of infections. We note that with increase in the values of α_1 and α_2 by greater margin, there is a huge fall in the total number of infected population. Use of face mask efficiently will help control the spread or virus in case of COVID-19 as well as the TB bacilli suspended in air in the form of droplet significantly. Fig. 3(b) shows that with increase in infection rates, the spread will be accelerated as higher infection rate imply occurrence of more effective contacts with infectious individuals. This needs to be taken seriously as this situation demands implementation of necessary interventions to reduce the spread of infection. Fig. 3(c) shows that if the immunity wanes quickly, the recoveries will reduce as this suggests that after recovery, the individuals soon become susceptible towards the disease again.

4.1. Sensitivity analysis

In this section we illustrate sensitivity analysis by means of forward sensitivity index [15] of the basic reproduction number (R_0) as well as we apply the approach of LHS-PRCC (i.e. Latin Hypercube Sampling - Partial Rank Correlation Coefficient) [11,32] on our model given by Eqs. (1)–(11) to study the influence on different infected population class of different parameters involved in the model. In the study [28], the authors worked on global dynamics of a HTLV-I infection model and have performed detailed sensitivity analysis by means of normalized forward sensitivity index to bring out the relative significance of certain parameters in disease transmission. Basic reproduction number (R_0) is very crucial in signifying the number the secondary cases arising from a single infected primary case and checks on whether the situation is under control or not. The normalized forward sensitivity index of a variable with respect to a parameter is the ratio of the relative change in the variable to the relative change in the parameter [15]. Therefore, if for say b represents a parameter, then the normalized forward sensitivity index of R_0 with respect to b is given by

$$r_b^{R_0} = \frac{\partial R_0}{\partial b} \times \frac{b}{R_0}.$$

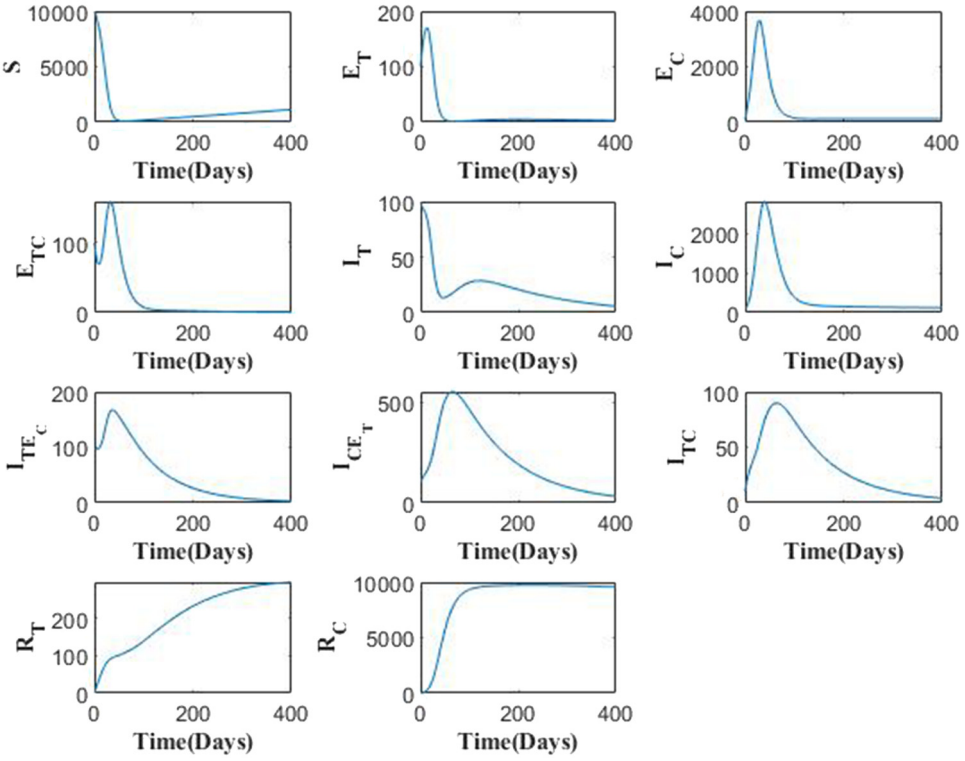

Fig. 2. Solution curves of the TB-COVID-19 co-infection model.

From Fig. 4 we note that R_0 shares negative indices with α_2 and γ_2 and positive indices with $\wedge$ and β_2. This implies the negative and positive correlation with the former and latter parameters respectively. This indicates that if larger fraction of population is using the mask efficiently then the spread of virus and the bacteria can be diminished. Higher recovery rates directly imply a shorter infectious period, which further suggests that period to make effective contacts is less, thereby reduction in the spread of infection and hence the basic reproduction number. In Fig. 4, the sensitivity indices respective to each parameter. These indices values further suggest that if there is a 10% increase in infection rate (β_2), then there will be a rise in the R_0 value by 10% as the respective index value is 1 for this parameter. In a similar way we note that the $r_{\gamma_2}^{R_0} = -0.99992$. This implies that a 10% increase in the recovery rate (γ_2) will decrease the R_0 by 9.9992%. Similarly it applies to the remaining set of parameters. In a similar context, we study the impact of two parameters at once on the basic reproduction number (R_0)in Fig. 5. Fig. 5(a) shows that with the increase in the infection rate (β_2), the R_0 value increases and it decreases with increase in α_2 value. Fig. 5(b) shows a similar behaviour with β_2 and γ_2. In Fig. 5(c) we clearly witness the decrease in the R_0 value with increase in face mask factor (α_2) and recovery rate (γ_2) values. This is evident as higher recovery rates implies shorter infectious period and thereby implying lesser chances of disease transmission. We obtain for a specific range of these parameters, the R_0 value can be brought below 1. The analysis on reproduction number is crucial as R_0 value is highly significant in determining the state of an epidemic. The value greater than 1 implies widespread of the disease in an uncontrolled manner. Hence from these two illustrations we conclude that usage of face mask correctly and efficiently will help in bringing down the basic reproduction number value thereby reducing the spread of disease vastly.

Sensitivity analysis following the approach of Latin Hypercube Sampling and Partial Rank Correlation Coefficient is employed to understand the complete parameter space on the different infected population variables of the model, and is illustrated in Fig. 6. The parameters are assumed to be uniformly distributed and the different response functions considered to perform the analysis are I_T, I_C, I_{TE_C}, I_{CE_T}, and I_{TC}. The effectiveness of this approach is tested by determining the PRCC values and further examining the sensitivity of the parameters of the developed model. To get the PRCC values, at first Latin Hypercube Sampling (LHS) method is applied to stratify the sample

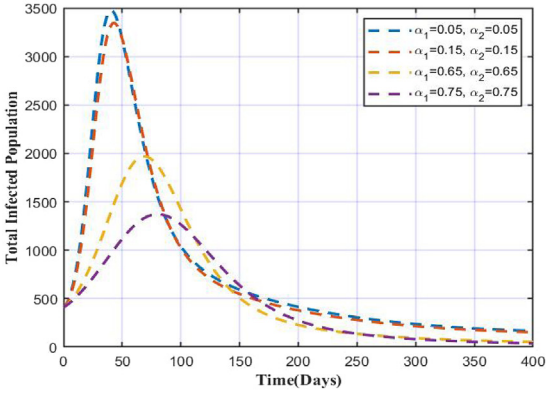

(a)

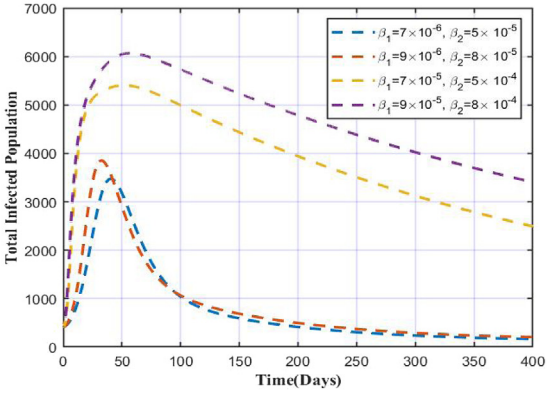

(b)

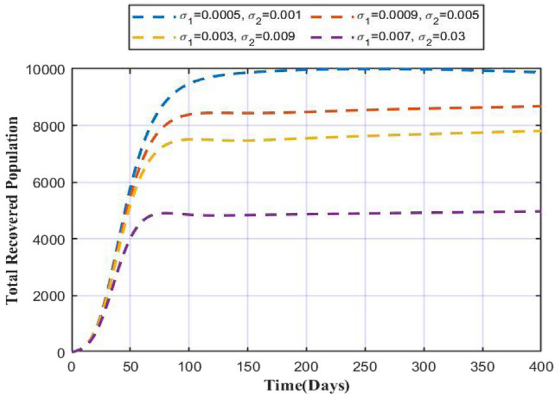

(c)

Fig. 3. Variation in total infected population with respect to (a) α_1, α_2, (b) β_1, β_2, and variation in total recovered population with respect to (c) σ_1, σ_2.

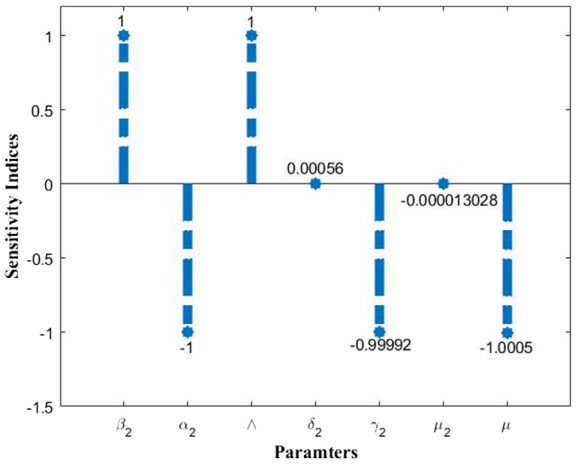

Fig. 4. Normalized forward sensitivity index of the basic reproduction number of the TB-COVID-19 co-infection model. The parameter values are as in Table 1.

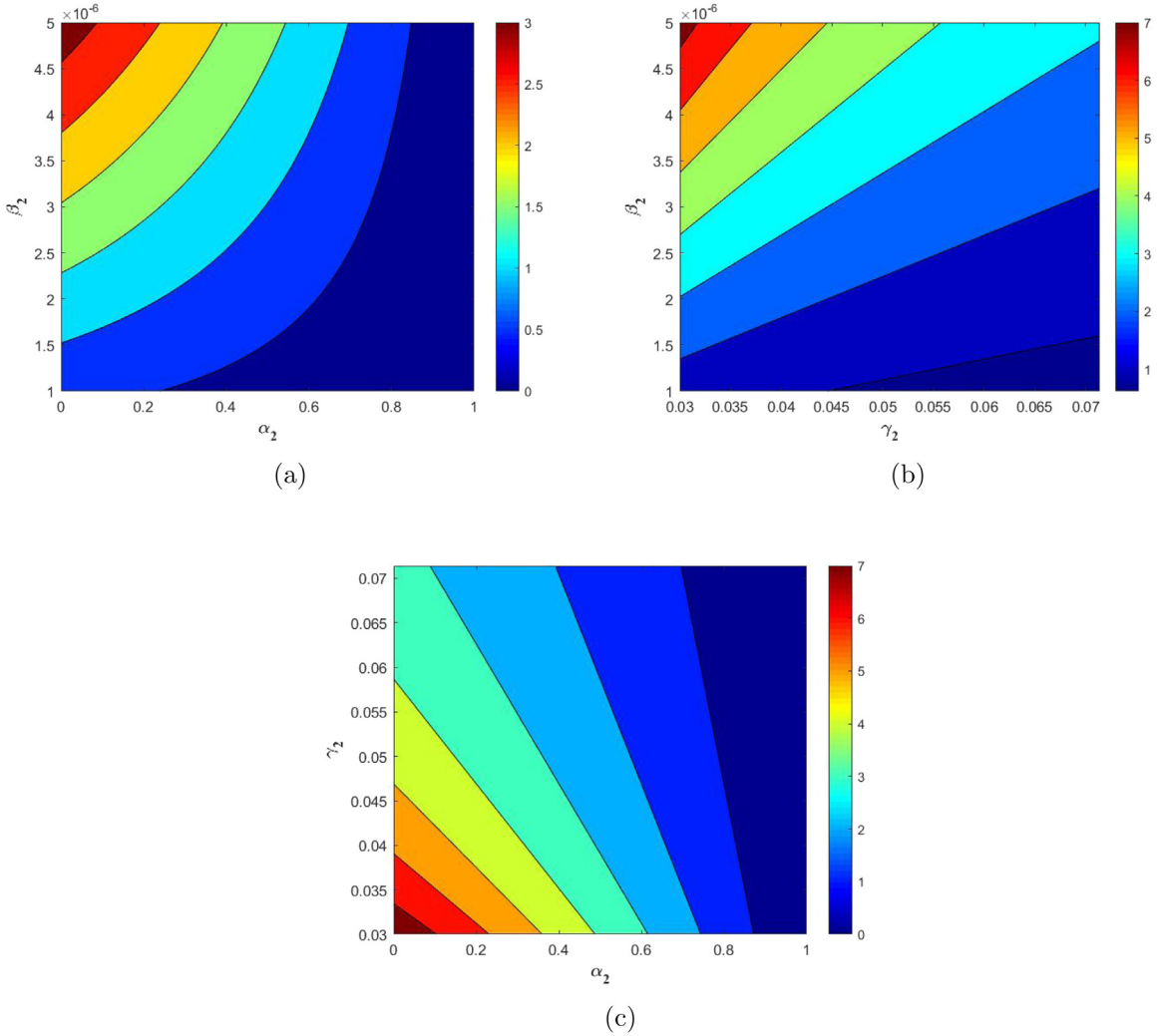

Fig. 5. Contour plots showing the effect of (a) β_2, α_2, (b) β_2, γ_2, and (c) γ_2, α_2 on the basic reproduction number.

without replacement. This is followed by setting the baseline values of the parameters and then the simulations are carried out for PRCC analysis. The set parameter values range between $\pm 25\%$ from the baseline value which are listed in Table 2, and the simulations are run for 500 days per LHS.

The PRCC value for each parameter corresponding to the respective response function is provided in Table 2. The magnitude as well as the direction of PRCC values of the distinct parameters are of prime importance in determining a respective parameter's contribution in model prediction and level of exactness. The PRCC values which are greater than 0.5 (closer to 1) and lesser than -0.5 (closer to -1) are quite important [45], as this implies stronger influence of LHS parameter on the outcome measure. From the Fig. 6, we clearly notice that the parameters β_1, β_2, γ_1, γ_2, η, η_2, ϵ_1, ϵ_2, ξ_1, ξ_2, σ_2, δ_1, δ_2 are having a stronger influence on each of the infected population considered. It is clearly observed that TB infection rate (β_1) has PRCC values very close to 1, signifying a higher level uncertainties or variations in infected population (I_T, I_{TE_C}, I_{CE_T} and I_{TC}) with change in its values. Surely, in case of the COVID-19 only infected population, the respective β_2 PRCC value is closer to 1 signifying a strong positive correlation. The similar explanation goes for the other such significant parameters. We observe that the recovery rates γ_1 and γ_2, and the enhancement factors ϵ_1, ϵ_2 and ϵ_3 have negative and positive PRCC values respectively with respect to the exposed and co-infected population I_{TE_C}, I_{CE_T} and I_{TC}. We also note that in each of these figures, either one of the parameters α_1 and α_2 or both which signify product of face mask efficacy and

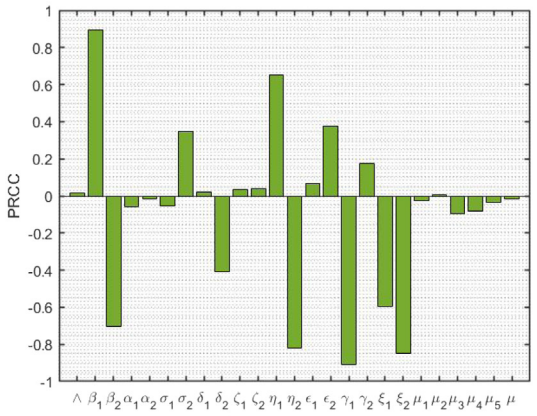

(a)

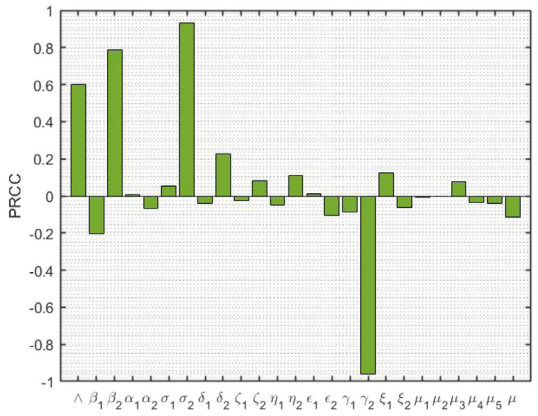

(b)

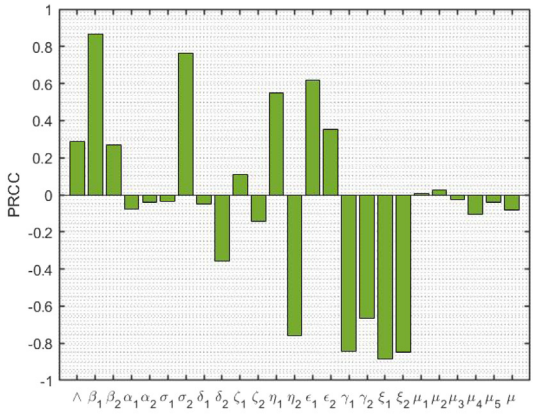

(c)

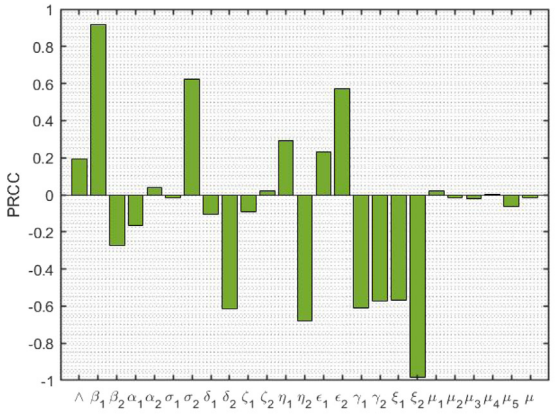

(d)

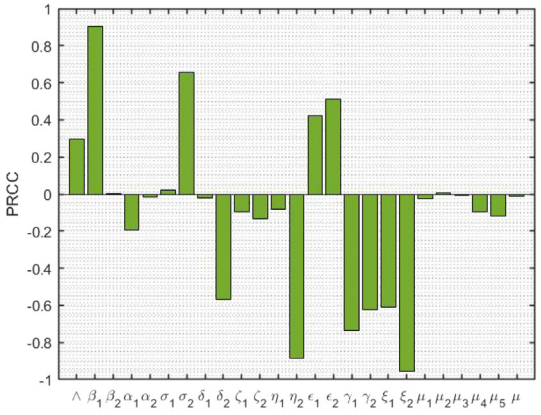

(e)

Fig. 6. PRCC results showing sensitivity indices of the model parameters with (a) TB only infected (I_T), (b) COVID-19 only infected (I_C), (c) TB infected COVID-19 exposed (I_{TE_C}), (d) COVID-19 infected TB exposed (I_{CE_T}), and (e) TB and COVID-19 co-infected (I_{TC}).

Table 2
PRCC values of the model parameters.

Parameters	Baseline value	Range	PRCC (I_T)	PRCC (I_C)	PRCC (I_{TE_C})	PRCC (I_{CE_T})	PRCC (I_{TC})
$\wedge$	2	1.5–2.5	0.0158	0.5987	0.2875	0.1962	0.2968
β_1	7×10^{-6}	5.25×10^{-6}–8.75×10^{-6}	0.8960	−0.2017	0.8655	0.9202	0.9060
β_2	5×10^{-5}	3.75×10^{-5}–6.25×10^{-5}	−0.7046	0.7854	0.2692	−0.2717	0.0020
α_1	0.05	0.0375–0.0625	−0.0567	0.0059	−0.0759	−0.1636	−0.1950
α_2	0.05	0.0375–0.0625	−0.0152	−0.0661	−0.0387	0.0402	−0.0156
σ_1	0.0005	3.75×10^{-4}–6.25×10^{-4}	−0.0541	0.0519	−0.0368	−0.0178	0.0210
σ_2	0.001	0.00075–0.0013	0.3499	0.9321	0.7623	0.6233	0.6571
δ_1	0.03	0.0225–0.0375	0.0227	−0.0410	−0.0481	−0.1052	−0.0189
δ_2	0.071	0.0532–0.0887	−0.4075	0.2250	−0.3565	−0.6160	−0.5699
ζ_1	0.01	0.0075–0.0125	0.0371	−0.0258	0.1113	−0.0902	−0.0950
ζ_2	0.07	0.0525–0.0875	0.0407	0.0816	−0.1442	0.0232	−0.1332
η_1	0.04	0.03–0.05	0.6535	−0.0468	0.5468	0.2936	−0.0807
η_2	0.0714	0.0536–0.0893	−0.8180	0.1113	−0.7595	−0.6782	−0.8872
ϵ_1	1.5	1.125–1.875	0.0681	0.0099	0.6170	0.2307	0.4251
ϵ_2	1.1	0.825–1.375	0.3765	−0.1046	0.3530	0.5742	0.5122
γ_1	0.04	0.03–0.05	−0.9093	−0.0857	−0.8418	−0.6079	−0.7352
γ_2	0.0714	0.0536–0.0893	0.1770	−0.9617	−0.6669	−0.5705	−0.6239
ξ_1	0.033	0.0248–0.0413	−0.5962	0.1245	−0.8860	−0.5685	−0.6096
ξ_2	0.01	0.0075–0.0125	−0.8501	−0.0614	−0.8481	−0.9849	−0.9549
μ_1	0.000069	5.175×10^{-5}–8.625×10^{-5}	−0.0267	−0.0055	0.0048	0.0225	−0.0234
μ_2	0.00008	6×10^{-5}–1×10^{-4}	0.0059	−0.0039	0.0256	−0.0151	0.0091
μ_3	0.00007	5.25×10^{-5}–8.75×10^{-5}	−0.0976	0.0787	−0.0238	−0.0197	−0.0077
μ_4	0.00009	6.75×10^{-5}–1.125×10^{-4}	−0.0828	−0.0372	−0.1033	0.0033	−0.0955
μ_5	0.00009	6.75×10^{-5}–1.125×10^{-4}	−0.0345	−0.0411	−0.0397	−0.0650	−0.1212
μ	0.0000425	3.1875×10^{-5}–5.3125×10^{-5}	−0.0156	−0.1137	−0.0828	−0.0172	−0.0099

fraction of population wearing it precisely, have negative PRCC values with respect to each infected population class, thereby signifying the crucial role of correct face mask usage in reduction of infections. The progression rates δ_1 and δ_2 are quite significant, since their values are either greater than 0.5 or lesser that -0.5, suggesting higher level of uncertainty in the rise and fall of the infected cases. Overall, we observe that the correlation between the respective variable and the parameter based on PRCC values, justifies with the respective model equations.

5. Optimal control

5.1. Optimal control problem

Optimal control analysis is of great importance in determining significant control strategies in infectious disease. As per the report by WHO [52], the TB care was reduced by 21% in low-income countries amid the COVID-19 pandemic. Since TB has a varied incubation as well as infectious period, in due time if treatment is provided and awareness is spread through counselling, risks related to chronic illness and development of COVID-19 disease along with TB can be avoided. It is also witnessed that COVID-19 can spread easily through the unidentified infectives. Therefore, it is of utmost significance for these exposed individuals to be isolated so that their contact with TB infectives can also be reduced. Being exposed to both of the diseases can be avoided if proper care is taken in controlling the spread of both diseases. Contemplating this, we include 2 control parameters in the TB-COVID-19 model represented by the system of Eqs. (1)–(11) which are:

- u_1: This control relates to improved and early detection of the exposed COVID-19 individuals by setting up rigorous testing drives, investing on home testing kits, and isolation facilities. This control is incorporated with a vision towards reduction of exposed COVID-19 individuals coming in contact with TB infected patients. This could help in reducing the population from getting exposed to both the diseases.
- u_2: This control relates towards improvement of TB recovery period. This is equated towards implementation of proper treatment and counselling policies for TB care, so that recovery period can be improved by providing right treatment and counselling at the initial stage, thereby reducing the negligence in taking treatment.

These two control functions are bounded and Lebesgue integrable on $[0, t_f]$, where t_f is the pre-fixed time period to which these two controls are applied. It is assumed that u_1 and u_2 lie between 0 and 1, the reason being, if these two equal zero, it simply infers no efforts being placed in these controls. Similarly, utmost effort implies to these values being 1. As per the above explanation we include the two controls in the model (1)–(11) and obtain the following optimal control model:

$$\frac{dS}{dt} = \wedge + \sigma_1 R_T + \sigma_2 R_C - (\lambda_T + \lambda_C + \mu)S \tag{17}$$

$$\frac{dE_T}{dt} = \lambda_T S - (\delta_1 + \lambda_C + \mu)E_T \tag{18}$$

$$\frac{dE_C}{dt} = \lambda_C S - (\delta_2 + \lambda_T(1 - u_1(t)) + \mu)E_C \tag{19}$$

$$\frac{dE_{TC}}{dt} = \lambda_C E_T + \lambda_T(1 - u_1(t))E_C - (\zeta_1 + \zeta_2 + \mu)E_{TC} \tag{20}$$

$$\frac{dI_T}{dt} = \delta_1 E_T + \eta_1 I_{TC} - (\epsilon_1\lambda_C + \mu_1 + \mu)I_T - (\gamma_1 + u_2(t))I_T \tag{21}$$

$$\frac{dI_C}{dt} = \delta_2 E_C + \eta_2 I_{TC} - (\gamma_2 + \epsilon_2\lambda_T + \mu_2 + \mu)I_C \tag{22}$$

$$\frac{dI_{TE_C}}{dt} = \epsilon_1\lambda_C I_T + \zeta_1 E_{TC} - (\xi_1 + \mu_3 + \mu)I_{TE_C} \tag{23}$$

$$\frac{dI_{CE_T}}{dt} = \epsilon_2\lambda_T I_C + \zeta_2 E_{TC} - (\xi_2 + \mu_4 + \mu)I_{CE_T} \tag{24}$$

$$\frac{dI_{TC}}{dt} = \xi_1 I_{TE_C} + \xi_2 I_{CE_T} - (\eta_1 + \eta_2 + +\mu_5 + \mu)I_{TC} \tag{25}$$

$$\frac{dR_T}{dt} = (\gamma_1 + u_2(t))I_T - (\sigma_1 + \mu)R_T \tag{26}$$

$$\frac{dR_C}{dt} = \gamma_2 I_C - (\sigma_2 + \mu)R_C, \tag{27}$$

where

$$\lambda_T = \beta_1(1 - \alpha_1)(I_T + I_{TC} + I_{TE_C}) \text{ and } \lambda_C = \beta_2(1 - \alpha_2)(I_C + I_{TC} + I_{CE_T})$$

The objective functional for the fixed t_f is given by

$$J = \int_0^{t_f} C_1 I_T + C_2 I_C + C_3 I_{TE_C} + C_4 I_{CE_T} + C_5 I_{TC} + \frac{1}{2}C_6 u_1^2 + \frac{1}{2}C_7 u_2^2, \tag{28}$$

where $C_1,\ C_2,\ C_3,\ C_4,\ C_5,\ C_6,\ C_7 \geq 0$ are the weight constants.

Objective is to find the control parameters u_1*, u_2* such that

$$J(u_1*, u_2*) = \min_{u_1, u_2 \in \Omega} J(u_1, u_2) \tag{29}$$

where Ω is the control set, defined as

$$\Omega = \{u_1, u_2 : \text{measurable} \quad \text{and} \quad 0 \leq u_1, u_2 < 1\} \quad \textit{and} \quad t \in [0, t_f]$$

The Lagrangian of this problem is:

$$L(I_T, I_C, I_{TE_C}, I_{CE_T}, I_{TC}, u_1, u_2) = C_1 I_T + C_2 I_C + C_3 I_{TE_C} + C_4 I_{CE_T} + C_5 I_{TC} + \frac{1}{2}C_6 u_1^2 + \frac{1}{2}C_7 u_2^2$$

The Hamiltonian $\mathcal{H}$ formed for our problem is :

$$\begin{aligned}\mathcal{H} = {} & (I_T, I_C, I_{TE_C}, I_{CE_T}, I_{TC}, u_1, u_2) + \lambda_1\frac{dS}{dt} + \lambda_2\frac{dE_T}{dt} + \lambda_3\frac{dE_C}{dt} + \lambda_4\frac{dE_{TC}}{dt} + \lambda_5\frac{dI_T}{dt} + \lambda_6\frac{dI_C}{dt} \\ & + \lambda_7\frac{dI_{TE_C}}{dt} + \lambda_8\frac{dI_{CE_T}}{dt} + \lambda_9\frac{dI_{TC}}{dt} + \lambda_{10}\frac{dR_T}{dt} + \lambda_{11}\frac{dR_C}{dt}\end{aligned}$$

where $\lambda_i's$ are the adjoint variables (i = 1 to 11). The adjoint variables are written in the form of differential equations as follows:

$$\frac{d\lambda_1}{dt} = -\frac{\partial \mathcal{H}}{\partial S} = (\lambda_1 - \lambda_2)\beta_1(1-\alpha_1)(I_T + T_{TC} + I_{TE_C}) + (\lambda_1 - \lambda_3)\beta_2(1-\alpha_2)(I_C + T_{TC} + I_{CE_T}) + \lambda_1\mu \tag{30}$$

$$\frac{d\lambda_2}{dt} = -\frac{\partial \mathcal{H}}{\partial E_T} = (\lambda_2 - \lambda_4)\beta_2(1-\alpha_2)(I_C + T_{TC} + I_{CE_T}) + (\lambda_2 - \lambda_5)\delta_1 + \lambda_2\mu \tag{31}$$

$$\frac{d\lambda_3}{dt} = -\frac{\partial \mathcal{H}}{\partial E_C} = (\lambda_3 - \lambda_4)(1-u_1(t))\beta_1(1-\alpha_1)(I_T + T_{TC} + I_{TE_C}) + (\lambda_3 - \lambda_6)\delta_2 + \lambda_3\mu \tag{32}$$

$$\frac{d\lambda_4}{dt} = -\frac{\partial \mathcal{H}}{\partial E_{TC}} = (\lambda_4 - \lambda_7)\zeta_1 + (\lambda_4 - \lambda_8)\zeta_2 + \lambda_4\mu \tag{33}$$

$$\frac{d\lambda_5}{dt} = -\frac{\partial \mathcal{H}}{\partial I_T} = -C_1 + (\lambda_1 - \lambda_2)\beta_1(1-\alpha_1)S + (\lambda_3 - \lambda_4)\beta_1(1-\alpha_1)(1-u_1(t))E_C + (\lambda_5 - \lambda_{10})(\gamma_1 + u_2(t)) + (\lambda_5 - \lambda_7)\epsilon_1\beta_2(1-\alpha_2)(I_C + T_{TC} + I_{CE_T}) + (\lambda_6 - \lambda_8)\epsilon_2\beta_1(1-\alpha_1)I_C + \lambda_5(\mu_1 + \mu) \tag{34}$$

$$\frac{d\lambda_6}{dt} = -\frac{\partial \mathcal{H}}{\partial I_C} = -C_2 + (\lambda_1 - \lambda_3)\beta_2(1-\alpha_2)S + (\lambda_2 - \lambda_4)\beta_2(1-\alpha_2)E_T + (\lambda_6 - \lambda_{11})\gamma_2 + (\lambda_5 - \lambda_7)\epsilon_1\beta_2(1-\alpha_2)I_T + (\lambda_6 - \lambda_8)\epsilon_2\beta_1(1-\alpha_1)(I_T + I_{TC} + I_{TE_C}) + \lambda_6(\mu_2 + \mu) \tag{35}$$

$$\frac{d\lambda_7}{dt} = -\frac{\partial \mathcal{H}}{\partial I_{TE_C}} = -C_3 + (\lambda_1 - \lambda_2)\beta_1(1-\alpha_1)S + (\lambda_3 - \lambda_4)\beta_1(1-\alpha_1)(1-u_1(t))E_C + (\lambda_6 - \lambda_8)\epsilon_2\beta_1(1-\alpha_1)I_C + (\lambda_7 - \lambda_9)\xi_1 + \lambda_7(\mu_3 + \mu) \tag{36}$$

$$\frac{d\lambda_8}{dt} = -\frac{\partial \mathcal{H}}{\partial I_{CE_T}} = -C_4 + (\lambda_1 - \lambda_3)\beta_2(1-\alpha_2)S + (\lambda_2 - \lambda_4)\beta_2(1-\alpha_2)E_T + (\lambda_8 - \lambda_9)\xi_2 + (\lambda_5 - \lambda_7)\epsilon_1\beta_2(1-\alpha_2)I_T + \lambda_8(\mu_4 + \mu) \tag{37}$$

$$\frac{d\lambda_9}{dt} = -\frac{\partial \mathcal{H}}{\partial I_{TC}} = -C_5 + (\lambda_1 - \lambda_2)\beta_1(1-\alpha_1)S + (\lambda_1 - \lambda_3)\beta_2(1-\alpha_2)S + (\lambda_3 - \lambda_4)\beta_1(1-\alpha_1)(1-u_1(t))E_C + (\lambda_2 - \lambda_4)\beta_2(1-\alpha_2)E_T + (\lambda_5 - \lambda_7)\epsilon_1\beta_2(1-\alpha_2)I_T + (\lambda_6 - \lambda_8)\epsilon_2\beta_1(1-\alpha_1)I_C + (\lambda_5 - \lambda_9)\eta_1 + (\lambda_6 - \lambda_9)\eta_2 + \lambda_9(\mu_5 + \mu) \tag{38}$$

$$\frac{d\lambda_{10}}{dt} = -\frac{\partial \mathcal{H}}{\partial R_T} = (\lambda_{10} - \lambda_1)\sigma_1 + \lambda_{10}\mu \tag{39}$$

$$\frac{d\lambda_{11}}{dt} = -\frac{\partial \mathcal{H}}{\partial R_C} = (\lambda_{11} - \lambda_1)\sigma_2 + \lambda_{11}\mu \tag{40}$$

Let $\widetilde{S}$, $\widetilde{E_T}$, $\widetilde{E_C}$, $\widetilde{E_{TC}}$, $\widetilde{I_T}$, $\widetilde{I_C}$, $\widetilde{I_{TE_C}}$, $\widetilde{I_{CE_T}}$, $\widetilde{I_T}$, $\widetilde{R_T}$, $\widetilde{R_C}$ be optimum values of S, E_T, E_C, E_{TC}, I_T, I_C, I_{TE_C}, I_{CE_T}, I_{TC}, R_T, and R_C respectively. Let $\widetilde{\lambda_1}$, $\widetilde{\lambda_2}$, $\widetilde{\lambda_3}$, $\widetilde{\lambda_4}$, $\widetilde{\lambda_5}$, $\widetilde{\lambda_6}$, $\widetilde{\lambda_7}$, $\widetilde{\lambda_8}$, $\widetilde{\lambda_9}$, $\widetilde{\lambda_{10}}$, and $\widetilde{\lambda_{11}}$ be solution of system of Eqs. (30)–(40). By using [30,36,37] we state and prove the below theorem.

Theorem 5.1. *There exist optimal controls $u_1*, u_2* \in \Omega$ such that $J(u_1*, u_2*) = \min J(u_1, u_2)$ subject to extended system of Eqs. (17)–(27).*

Proof. We use [37] to prove this theorem. In this case, we observe that the controls are non-negative. The necessary convexity of the objective functional in (u_1, u_2) is satisfied for minimizing the problem. The set of control variable, $u_1, u_2 \in \Omega$ is convex and closed by definition. The state variables are bounded and the integrand of the functional $C_1I_T + C_2I_C + C_3I_{TE_C} + C_4I_{CE_T} + C_5I_{TC} + \frac{1}{2}C_6u_1^2 + \frac{1}{2}C_7u_2^2$ is convex on Ω. Since there exist optimal controls for minimizing the functional subject to systems (17)–(27) and (30)–(40), we use Pontryagin's maximum principle [37] to derive the necessary conditions to find the optimal solutions in the following way: Suppose (z, u) is an optimal solution of an optimal control problem, then this implies that there exists a non-trivial vector function

$\lambda = \lambda_1, \lambda_2, \ldots, \lambda_n$ satisfying the following:

$$\frac{dz}{dt} = \frac{\partial \mathcal{H}(t,z,u,\lambda)}{\partial \lambda}, \quad 0 = \frac{\partial \mathcal{H}(t,z,u,\lambda)}{\partial u} \text{ at } u*, \quad \frac{d\lambda}{dt} = -\frac{\partial \mathcal{H}(t,z,u,\lambda)}{\partial z}$$

Theorem 5.2. *The optimal controls u_1*, u_2* which minimize J over the region Ω is given by:*

$$u_1* = \min\{1, \max(0, \widetilde{u_1})\} \quad \textit{and} \quad u_2* = \min\{1, \max(0, \widetilde{u_2})\},$$

where

$$\widetilde{u_1} = \frac{(\lambda_3 - \lambda_4)\beta_1(1-\alpha_1)(I_T + I_{TC} + T_{TE_C})E_C}{C_6} \textit{ and } \widetilde{u_2} = \frac{(\lambda_5 - \lambda_{10})I_T}{C_7}$$

Proof. We prove this theorem by using [36,37] and Theorem 5.1.

Using the optimally condition: $\frac{\partial \mathcal{H}}{\partial u_1} = 0$, $\frac{\partial \mathcal{H}}{\partial u_2} = 0$ we get,

$$\frac{\partial \mathcal{H}}{\partial u_1} = C_6 u_1 + (\lambda_3 - \lambda_4)\beta_1(1-\alpha_1)(I_T + I_{TC} + T_{TE_C})E_C = 0$$

$$\implies u_1 = \frac{(\lambda_3 - \lambda_4)\beta_1(1-\alpha_1)(I_T + I_{TC} + T_{TE_C})E_C}{C_6} = \widetilde{u_1}$$

$$\text{and} \quad \frac{\partial \mathcal{H}}{\partial u_2} = C_7 u_2 + (\lambda_5 - \lambda_{10})I_T = 0$$

$$\implies u_2 = \frac{(\lambda_5 - \lambda_{10})I_T}{C_7} = \widetilde{u_2}$$

Again the lower bound is 0 and upper bound is 1 for the controls u_1 and u_2. This suggests that $u_1 = u_2 = 0$ if $\widetilde{u_1} < 0$ and $\widetilde{u_2} < 0$, also $u_1 = u_2 = 1$ if $\widetilde{u_1} > 1$ and $\widetilde{u_2} > 1$, otherwise $u_1 = \widetilde{u_1}$ and $u_2 = \widetilde{u_2}$. Therefore, for these controls u_1* and u_2* we get optimum values of J.

5.2. Optimal control model simulation

In this section we perform simulations for a period of 400 days and illustrate analytical results using MATLAB software, by setting the parameter values as in Table 1. The extended system of Eqs. (17)–(27) is solved applying iterative method using forward and backward difference approximation as in [30]. The forward difference approximation is applied to first solve the state equations (17)–(27), and then applying the backward difference approximation, the adjoint equations (30)–(40) are solved. The positive valued constants C_1, C_2, C_3, C_4, C_5 are the weight constants which represent the weight which balance offs the TB only infected population, COVID-19 only infected population, TB infected COVID-19 exposed population, COVID-19 infected TB exposed population, and co-infected population to both the diseases respectively. The positive constants C_6, and C_7 represent the weight constants for improved testing and TB treatment, counselling respectively. The values assigned to the weight constants are $C_1 = 1$, $C_2 = 1$, $C_3 = 1$, $C_4 = 1$, $C_5 = 1$, $C_6 = 100$, and $C_7 = 100$. The initial values assigned to the variables to perform the simulations are $S = 10000$, $E_T = 100$, $E_C = 100$, $E_{TC} = 100$, $I_T = 100$, $I_C = 100$, $I_{TE_C} = 100$, $I_{CE_T} = 100$, $I_{TC} = 10$, $R_T = 1$, $R_C =$ ‘1. In this section, the impact on control profile with variation in costs is studied. This is followed by studying the impact on the infected population with and without the two controls as well considering specifically one control at a time.

The illustration on the control profiles over time as well the impact on the same due to variation in costs is depicted in Fig. 7. It is clearly observed that the control u_2 needs to be maintained at 1 for longer time compared to that of control u_1, implying that significance of control u_2 is more compared to that of u_1. From Fig. 7(c) and (d) we observe that with the increase in the costs, the duration for which the control profile resides at 1 declines. This is justified, as higher costs in the means of providing testing kits, conducting testing drives, counselling and treatment facilities etc. call in for lesser duration of investments on those equipment and policies. In the coming section we see the variation in infected population with and without application of controls parameters, and provide a clarity on the significance of the controls individually as well as when applied together.

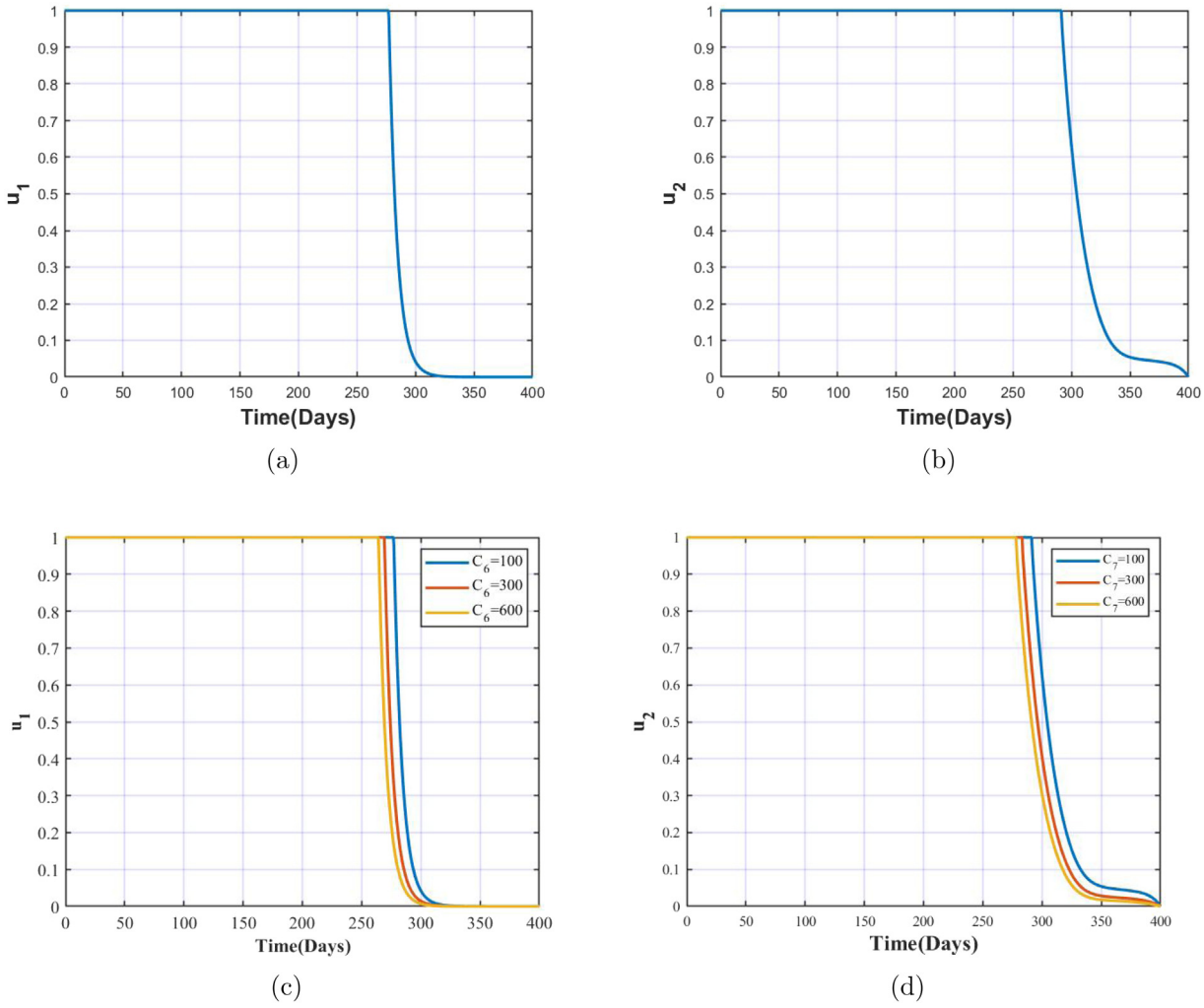

Fig. 7. Control profile of (a) u_1, (b) u_2, (c) u_1 with variation in costs and (d) u_2 with variation in costs.

5.2.1. Optimal control simulation when both controls are applied

When both controls relating to enhanced detection and isolation (i.e. $u_1 \neq 0$) and early TB treatment and counselling (i.e. $u_2 \neq 0$) are applied, it results in significant difference in the number of infectives under the application of controls which is depicted in Fig. 8. We note that for each class of infected population there is huge decrease in the number of infectives when both controls are applied, and the number nears to zero in a shorter period of time, except for COVID-19 only infected population. In the later case there is a very small difference, since the controls focus on minimizing exposure to both diseases with major insistence on TB treatment. As per the report [52] and the study in [14], it is conveyed that the TB infected individuals, both latent TB patients as well as with TB disease are at increased risk of getting COVID-19 as well as the severity of the COVID-19 symptoms in these patients would be more. Hence, our optimal control model which was framed keeping this into consideration provides desired results, stressing on the importance of both the control parameters when implemented at once.

5.2.2. Optimal control simulation when exclusively one of the controls is applied

In the case when $u_1 = 0$ and only the control related to improved TB treatment and counselling ($u_2 \neq 0$) is applied we see that there is a considerable decline in the number of infectives of each class when the control is

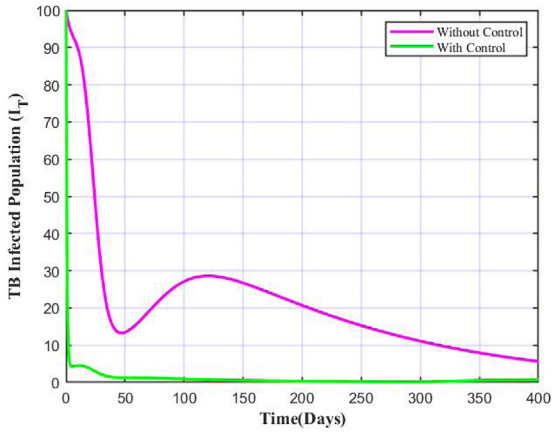

(a)

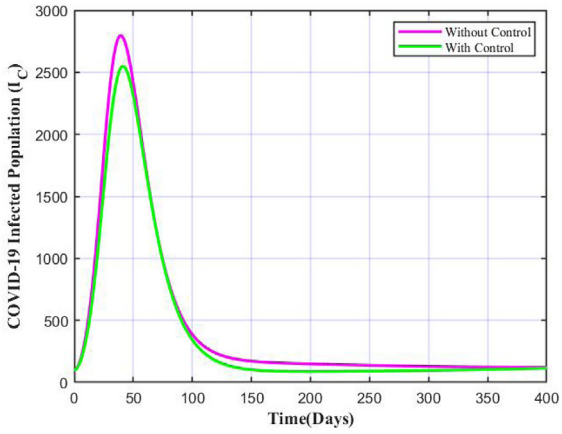

(b)

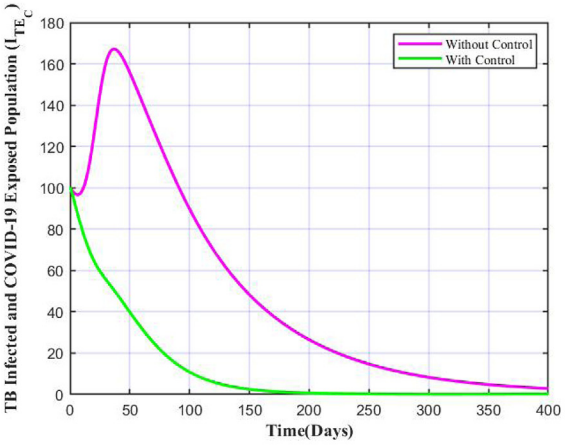

(c)

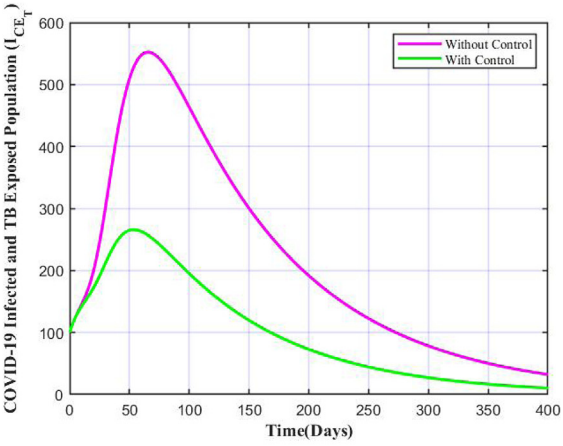

(d)

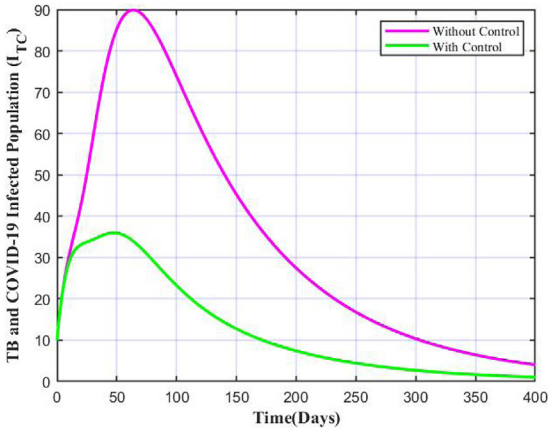

(e)

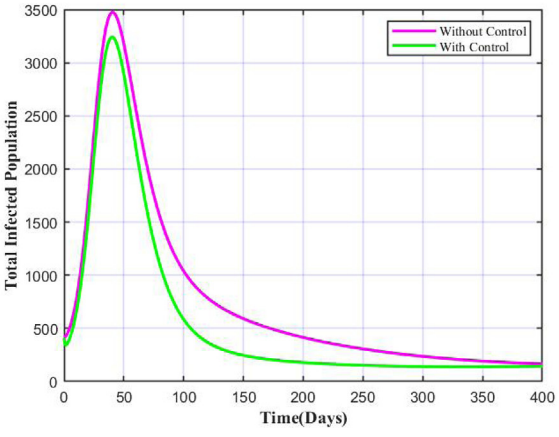

(f)

Fig. 8. Variation in infected population with and without both the controls.

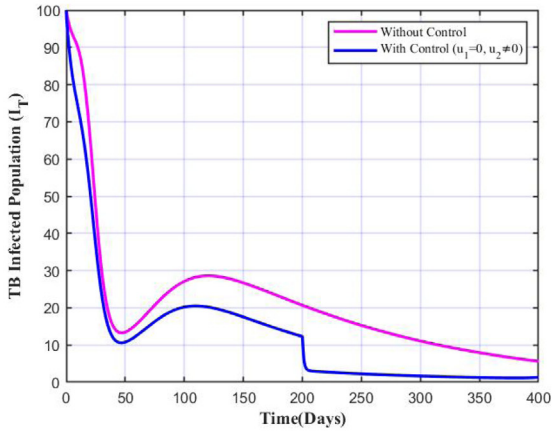

(a)

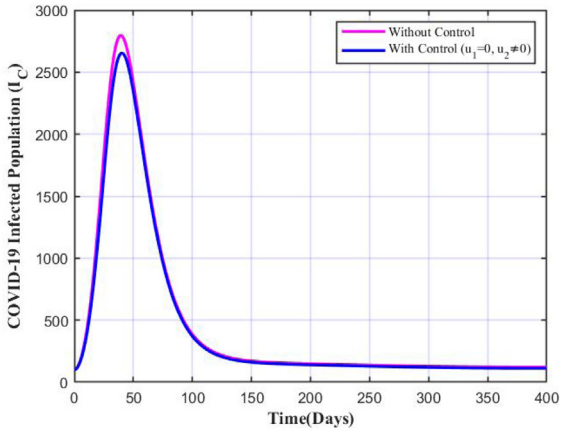

(b)

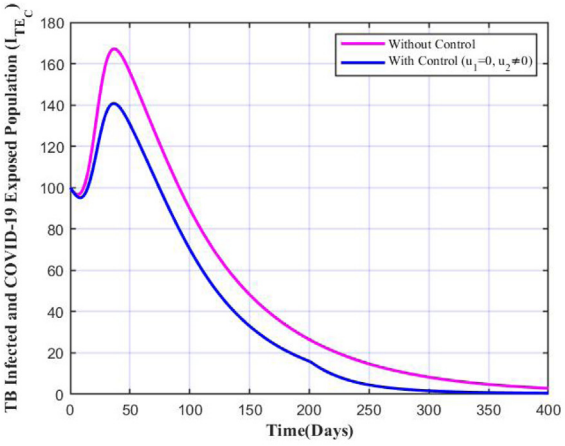

(c)

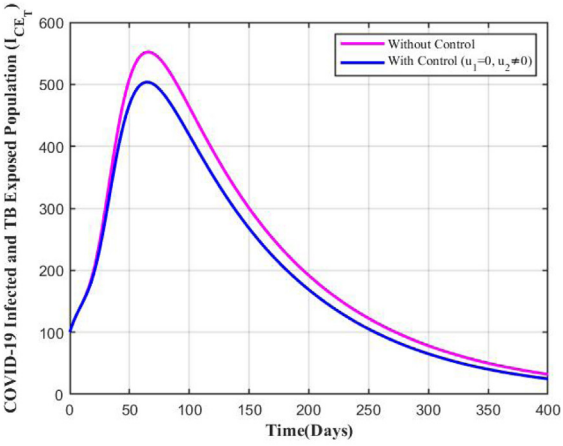

(d)

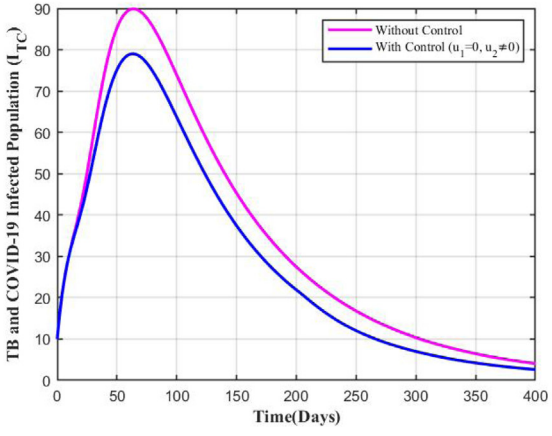

(e)

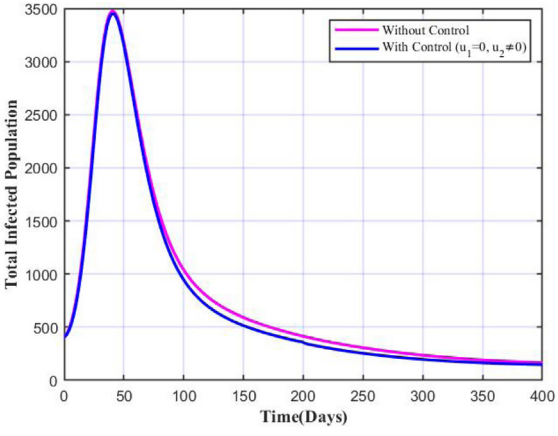

(f)

Fig. 9. Variation in infected population with TB treatment and counselling ($u_2 \neq 0,\ u_1 = 0$) control only.

applied which is shown in Fig. 9. This suggests that the control u_2 is quite important in controlling the disease spread, since even when implemented alone it contributes towards reduction of infected cases. This is supported by the studies [14,52] which suggests that TB infected patients are more vulnerable to COVID-19, implying higher individuals with dual infections. On the other hand, from the Fig. 10 we note that there is barely any difference in number of infectives with and without the control u_1. This suggests that without improved TB care ($u_2 = 0$) and mere detection and isolation of exposed COVID-19 individuals ($u_1 \neq 0$) will not help in decline of co-infections, single disease infection or simultaneous infection from one disease and exposure to another disease as per our model. Though the control u_1 is not significant compared to the control u_2 when applied separately, however when both controls are applied at once we notice that the decline in number of infected population is much higher when mere one control is applied. Therefore, these simulations stress on the importance of both the controls in controlling spread of co-infections when implemented together.

6. Conclusion

In this work we performed a detailed study on the deterministic epidemiological model comprising of 11 compartments. The study began with a detailed analysis covering equilibria, basic reproduction number, stability and bifurcation analysis of the disease-free and endemic equilibrium. From the analysis on TB only model and COVID-19 only model we prove that the disease-free equilibrium and the endemic equilibrium are locally asymptotically stable when the respective basic reproduction numbers (R_{0_T} and R_{0_C}) are less than 1 and greater than 1 respectively. It is concluded that backward bifurcation does not exist in both models by applying centre manifold theory as in [13]. We obtain 4 equilibria for the TB - COVID-19 complete model, which are the disease-free equilibrium point, TB only equilibrium point, COVID-19 only equilibrium point and TB - COVID-19 co-existence endemic equilibrium point. The stability and bifurcation analysis are shown which prove the non-existence of backward bifurcation at $R_0 = 1$. These theoretical results are then followed by numerical simulations, sensitivity analysis and optimal control analysis.

Time series behaviour of the total infected and total recovered population for a period of 400 days is studied with respect to variation in two parameters at once, and it is witnessed that with increase in face mask efficacy and fraction of population wearing it precisely, the infection spread can be curbed. On the other hand, if the immunity wanes quickly, the recovered individuals move to being susceptible and hence at risk of infections. We note that with increase in recovery rates, the number of infected reduces, since smaller recovery implies shorter infectious period thereby nullifying the chance of spreading infections. Similarly, the impact of recovery rate, infection rate and face mask factor on the basic reproduction number is illustrated through sensitivity analysis and similar results are obtained. Using LHS-PRCC approach the significance and correlation of all the parameters with their respective response functions which in our case of study were the different infected population classes were obtained and analysed based on the PRCC values.

Optimal control analysis was then performed by including two control parameters, one is the enhanced detection and isolation ($u_1(t)$) and the other is early TB treatment and counselling (i.e. $u_2(t)$). A significant difference in the number of infectives under the application of controls was witnessed in the illustration. The effect of these controls individually was also performed and when compared, the control $u_2(t)$ served to be more important than $u_1(t)$, but when applied together, the reduction in the number of infected population was quite huge. Therefore, going by the study in [14] and the report by WHO [52] both latent TB patients as well as with TB disease are at increased risk of getting COVID-19. The controls which were included in the study provided desired results so as to combat the challenge of co-infection of these disease spread. Hence, this analysis focused on the need of improved TB treatment and care as well as enhanced testing and isolation facilities for COVID-19 exposed population to combat the unforeseen spread of two deadly diseases. Hence, the results from the study implies acceleration in the disease spread if proper treatment and care for TB infectives is neglected and detection, isolation facilities are not implemented. On a concluding note, the study further suggests that in the times of a pandemic, other chronic diseases, specifically the ones which spread through close contacts must not be neglected and adequate care has to be taken so that mortality due to co-infection and unavailability of timely treatment can be avoided.

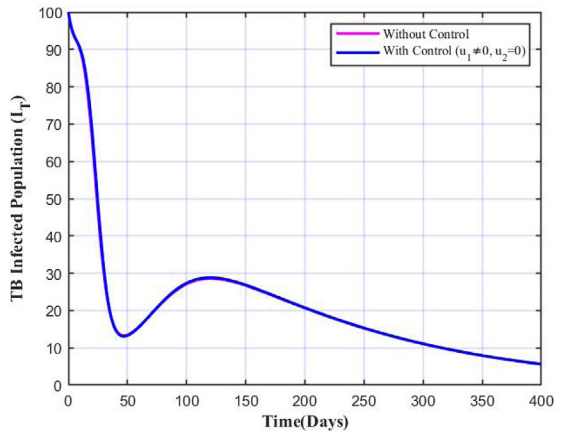

(a)

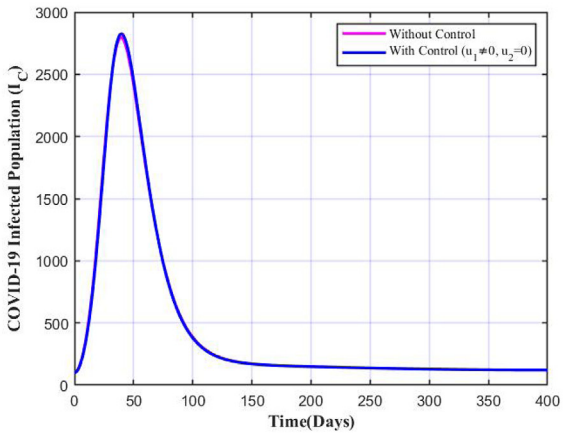

(b)

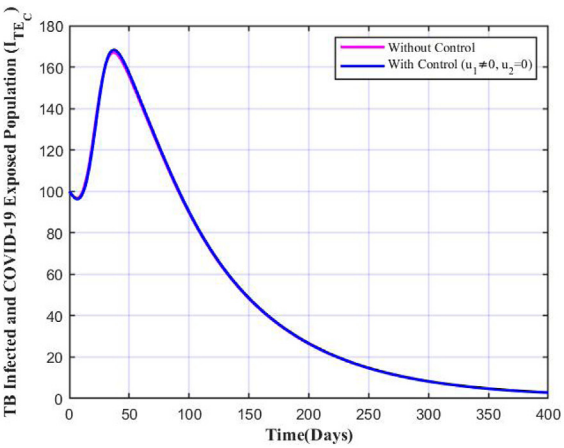

(c)

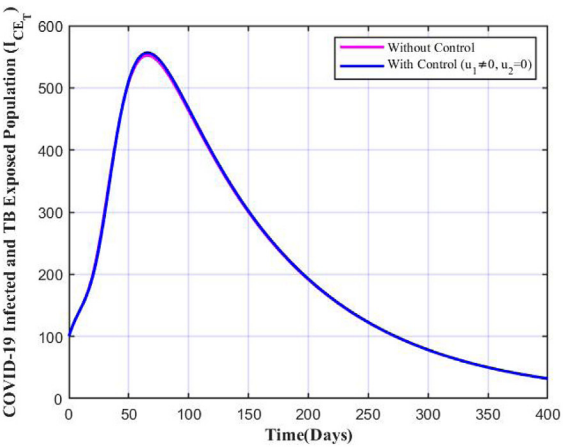

(d)

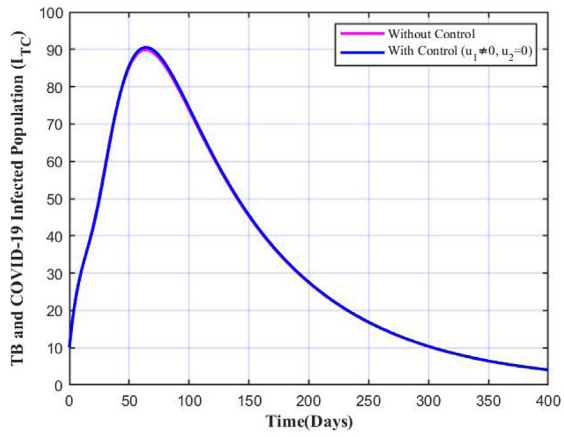

(e)

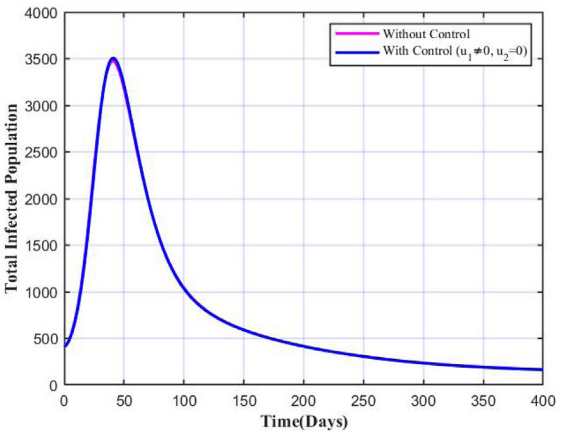

(f)

Fig. 10. Variation in infected population with testing drives for detection of exposed COVID-19 cases ($u_1 \neq 0,\ u_2 = 0$) control only.

Declaration of competing interest

The authors declare that they have no known competing financial interests or personal relationships that could have appeared to influence the work reported in this paper.

Acknowledgements

The authors extend their gratitude towards the reviewer and editor for their valuable suggestions in improvising the manuscript.

Appendix

Theorem A.1 (*Castillo-Chavez and Song*)**.** *Consider the following general system of ordinary differential equations with a parameter ϕ:*

$$\frac{dx}{dt} = f(x, \phi), \quad f : \mathbb{R}^n \times \mathbb{R} \to \mathbb{R} \ \text{ and } \ C^2(\mathbb{R}^n \times \mathbb{R}) \tag{41}$$

where 0 is an equilibrium point of the system that is, $f(0, \phi) \equiv 0$ for all ϕ and assume

1. *$A = D_x f(0, 0) = \left(\frac{\partial f_i}{\partial x_j}(0, 0)\right)$ is the linearization matrix of system (2) around the equilibrium 0 and ϕ evaluated at 0. Zero is a simple eigenvalue of A and other eigenvalues of A have negative real parts;*
2. *Matrix A has a right eigenvector W and a left eigenvector V (each corresponding to the zero eigenvalue); Let f_k be the kth component of f and*

$$a = \sum_{k,j,i=1}^{n} v_k w_i w_j \frac{\partial^2 f_k}{\partial x_i \partial x_j}(0, 0), \quad b = \sum_{k,i=1}^{n} v_k w_i \frac{\partial^2 f_k}{\partial x_i \partial \phi}(0, 0)$$

The local dynamics of the system around 0 is totally determined by the signs of a and b.

1. *$a > 0$, $b > 0$. When $\phi < 0$ with $| \phi | \ll 1$, 0 is locally asymptotically stable and there exists a positive unstable equilibrium; when $0 < \phi \ll 1$, 0 is unstable and there exists a negative, locally asymptotically stable equilibrium;*
2. *$a < 0$, $b < 0$. When $\phi < 0$ with $| \phi | \ll 1$, 0 is unstable; when $0 < \phi \ll 1$, 0 is locally asymptotically stable and there exists a positive unstable equilibrium;*
3. *$a > 0$, $b < 0$. When $\phi < 0$ with $| \phi | \ll 1$, 0 is unstable and there exists a locally asymptotically stable negative equilibrium; when $0 < \phi \ll 1$, 0 is stable and a positive unstable equilibrium appears;*
4. *$a\langle 0$, $b\rangle 0$. When ϕ changes from negative to positive, 0 changes its stability from stable to unstable. Correspondingly a negative unstable equilibrium becomes positive and locally asymptotically stable.*

References

[1] URL: https://www.who.int/health-topics/coronavirus.
[2] URL: https://covid19.who.int/.
[3] URL: https://www.worldometers.info/coronavirus/country/india/.
[4] URL: https://tbfacts.org/tb-statistics-india/.
[5] URL: https://hub.tbdiah.org/dashboards/countries/India.
[6] URL: https://worldhealthorg.shinyapps.io/tb_pronto/.
[7] S.R. Bandekar, M. Ghosh, Mathematical modeling of COVID-19 in India and its states with optimal control, Model. Earth Syst. Environ. (2021) http://dx.doi.org/10.1007/s40808-021-01202-8.
[8] S.R. Bandekar, M. Ghosh, Modeling and analysis of COVID-19 in India with treatment function through different phases of lockdown and unlock, Stoch. Anal. Appl. (2021) 1–18, http://dx.doi.org/10.1080/07362994.2021.1962343.
[9] A. Bandyopadhyay, S. Palepu, K. Bandyopadhyay, S. Handu, COVID-19 and tuberculosis co-infection: a neglected paradigm, Monaldi Arch. Chest Dis. 90 (3) (2020) http://dx.doi.org/10.4081/monaldi.2020.1437.
[10] I. Barberis, N.L. Bragazzi, L. Galluzzo, M. Martini, The history of tuberculosis: from the first historical records to the isolation of Koch's bacillus, J. Prev. Med. Hyg. (ISSN: 1121-2233) 58 (2017) E9–E12.
[11] S.M. Blower, H. Dowlatabadi, Sensitivity and uncertainty analysis of complex models of disease transmission: An HIV model, as an example, Int. Stat. Rev. / Rev. Int. Stat. 62 (2) (1994) 229, http://dx.doi.org/10.2307/1403510.
[12] J. Carr, Applications of Centre Manifold Theory, Springer US, 1981, http://dx.doi.org/10.1007/978-1-4612-5929-9.

[13] C. Castillo-Chavez, B. Song, Dynamical models of tuberculosis and their applications, Math. Biosci. Eng. 1 (2) (2004) 361–404, http://dx.doi.org/10.3934/mbe.2004.1.361.
[14] Y. Chen, Y. Wang, J. Fleming, Y. Yu, Y. Gu, C. Liu, L. Fan, X. Wang, M. Cheng, L. Bi, Y. Liu, Active or latent tuberculosis increases susceptibility to COVID-19 and disease severity, 2020, http://dx.doi.org/10.1101/2020.03.10.20033795.
[15] N. Chitnis, J.M. Hyman, J.M. Cushing, Determining important parameters in the spread of malaria through the sensitivity analysis of a mathematical model, Bull. Math. Biol. 70 (5) (2008) 1272–1296, http://dx.doi.org/10.1007/s11538-008-9299-0.
[16] D.K. Das, S. Khajanchi, T.K. Kar, The impact of the media awareness and optimal strategy on the prevalence of tuberculosis, Appl. Math. Comput. 366 (2020) 124732, http://dx.doi.org/10.1016/j.amc.2019.124732.
[17] D.K. Das, S. Khajanchi, T.K. Kar, Transmission dynamics of tuberculosis with multiple re-infections, Chaos Solitons Fractals 130 (2020) 109450, http://dx.doi.org/10.1016/j.chaos.2019.109450.
[18] K. Das, B. Murthy, S.A. Samad, M.H.A. Biswas, Mathematical transmission analysis of SEIR tuberculosis disease model, Sens. Int. 2 (2021) 100120, http://dx.doi.org/10.1016/j.sintl.2021.100120.
[19] A. Davies, K.-A. Thompson, K. Giri, G. Kafatos, J. Walker, A. Bennett, Testing the efficacy of homemade masks: Would they protect in an influenza pandemic? Disaster Med. Public Health Prep. 7 (4) (2013) 413–418, http://dx.doi.org/10.1017/dmp.2013.43.
[20] O. Diekmann, J. Heesterbeek, J. Metz, On the definition and the computation of the basic reproduction ratio R0 in models for infectious diseases in heterogeneous populations, J. Math. Biol. 28 (1990) 365–382.
[21] S.E. Eikenberry, M. Mancuso, E. Iboi, T. Phan, K. Eikenberry, Y. Kuang, E. Kostelich, A.B. Gumel, To mask or not to mask: Modeling the potential for face mask use by the general public to curtail the COVID-19 pandemic, Infect. Dis. Model. 5 (2020) 293–308, http://dx.doi.org/10.1016/j.idm.2020.04.001.
[22] Z. Feng, C. Castillo-Chavez, A.F. Capurro, A model for tuberculosis with exogenous reinfection, Theor. Popul. Biol. 57 (3) (2000) 235–247, http://dx.doi.org/10.1006/tpbi.2000.1451.
[23] N. Ferguson, D. Laydon, G. Nedjati Gilani, N. Imai, K. Ainslie, M. Baguelin, S. Bhatia, A. Boonyasiri, Z.U.L.M.A. Cucunuba Perez, G. Cuomo-Dannenburg, A. Dighe, I. Dorigatti, H. Fu, K. Gaythorpe, W. Green, A. Hamlet, W. Hinsley, L. Okell, S. Van Elsland, H. Thompson, R. Verity, E. Volz, H. Wang, Y. Wang, P. Walker, P. Winskill, C. Whittaker, C. Donnelly, S. Riley, A. Ghani, Report 9: Impact of non-pharmaceutical interventions (NPIs) to reduce COVID19 mortality and healthcare demand, 2020, http://dx.doi.org/10.25561/77482.
[24] Global Tuberculosis Report, Tech. rep., World Health Organization, 2020, URL: https://apps.who.int/iris/bitstream/handle/10665/336069/9789240013131-eng.pdf.
[25] H.W. Hethcote, Qualitative analyses of communicable disease models, Math. Biosci. 28 (3–4) (1976) 335–356, http://dx.doi.org/10.1016/0025-5564(76)90132-2.
[26] B. Ivorra, M. Ferrández, M. Vela-Pérez, A. Ramos, Mathematical modeling of the spread of the coronavirus disease 2019 (COVID-19) taking into account the undetected infections. The case of China, Commun. Nonlinear Sci. Numer. Simul. 88 (2020) 105303, http://dx.doi.org/10.1016/j.cnsns.2020.105303.
[27] W.O. Kermack, A.G. McKendrick, A contribution to the mathematical theory of epidemics, Proc. R. Soc. A 115 (772) (1927) 700–721, http://dx.doi.org/10.1098/rspa.1927.0118.
[28] S. Khajanchi, S. Bera, T.K. Roy, Mathematical analysis of the global dynamics of a HTLV-I infection model, considering the role of cytotoxic T-lymphocytes, Math. Comput. Simulation 180 (2021) 354–378, http://dx.doi.org/10.1016/j.matcom.2020.09.009.
[29] S.A. Lauer, K.H. Grantz, Q. Bi, F.K. Jones, Q. Zheng, H.R. Meredith, A.S. Azman, N.G. Reich, J. Lessler, The incubation period of coronavirus disease 2019 (COVID-19) from publicly reported confirmed cases: Estimation and application, Ann. Internal Med. 172 (9) (2020) 577–582, http://dx.doi.org/10.7326/m20-0504.
[30] S. Lenhart, J.T. Workman, Optimal Control Applied to Biological Models, CRC Press, Boca Raton, 2007.
[31] R. Li, S. Pei, B. Chen, Y. Song, T. Zhang, W. Yang, J. Shaman, Substantial undocumented infection facilitates the rapid dissemination of novel coronavirus (SARS-CoV-2), Science 368 (6490) (2020) 489–493, http://dx.doi.org/10.1126/science.abb3221.
[32] S. Marino, I.B. Hogue, C.J. Ray, D.E. Kirschner, A methodology for performing global uncertainty and sensitivity analysis in systems biology, J. Theoret. Biol. 254 (1) (2008) 178–196, http://dx.doi.org/10.1016/j.jtbi.2008.04.011.
[33] S. Mushayabasa, E.T. Ngarakana-Gwasira, J. Mushanyu, On the role of governmental action and individual reaction on COVID-19 dynamics in South Africa: A mathematical modelling study, Inform. Med. Unlocked (2020) 100387, http://dx.doi.org/10.1016/j.imu.2020.100387.
[34] C.N. Ngonghala, E. Iboi, S. Eikenberry, M. Scotch, C.R. MacIntyre, M.H. Bonds, A.B. Gumel, Mathematical assessment of the impact of non-pharmaceutical interventions on curtailing the 2019 novel Coronavirus, Math. Biosci. 325 (2020) 108364, http://dx.doi.org/10.1016/j.mbs.2020.108364.
[35] M. Nicola, Z. Alsafi, C. Sohrabi, A. Kerwan, A. Al-Jabir, C. Iosifidis, M. Agha, R. Agha, The socio-economic implications of the coronavirus pandemic (COVID-19): A review, Int. J. Surg. 78 (2020) 185–193, http://dx.doi.org/10.1016/j.ijsu.2020.04.018.
[36] L.S. Pontryagin, Mathematical Theory of Optimal Processes, in: Classics of Soviet Mathematics, Taylor & Francis, ISBN: 9782881240775, 1987, URL: https://books.google.co.in/books?id=kwzq0F4cBVAC.
[37] L.S. Pontryagin, V.G. Boltyanskii, R.V. Gamkrelidze, E.F. Mishchenko, The Mathematical Theory of Optimal Processes, Wiley, New York, 1962.
[38] T.C. Porco, S.M. Blower, Quantifying the intrinsic transmission dynamics of tuberculosis, Theor. Popul. Biol. 54 (2) (1998) 117–132, http://dx.doi.org/10.1006/tpbi.1998.1366.
[39] R.K. Rai, S. Khajanchi, P.K. Tiwari, E. Venturino, A.K. Misra, Impact of social media advertisements on the transmission dynamics of COVID-19 pandemic in India, J. Appl. Math. Comput. 68 (1) (2021) 19–44, http://dx.doi.org/10.1007/s12190-021-01507-y.
[40] K. Sarkar, S. Khajanchi, J.J. Nieto, Modeling and forecasting the COVID-19 pandemic in India, Chaos Solitons Fractals 139 (2020) 110049, http://dx.doi.org/10.1016/j.chaos.2020.110049.

[41] S. Scheiner, N. Ukaj, C. Hellmich, Mathematical modeling of COVID-19 fatality trends: Death kinetics law versus infection-to-death delay rule, Chaos Solitons Fractals 136 (2020) 109891, http://dx.doi.org/10.1016/j.chaos.2020.109891.
[42] A.K. Srivastav, M. Ghosh, S.R. Bandekar, Modeling of COVID-19 with limited public health resources: a comparative study of three most affected countries, Eur. Phys. J. Plus 136 (4) (2021) http://dx.doi.org/10.1140/epjp/s13360-021-01333-y.
[43] K.T.L. Sy, N.J.L. Haw, J. Uy, Previous and active tuberculosis increases risk of death and prolongs recovery in patients with COVID-19, Infect. Dis. 52 (12) (2020) 902–907, http://dx.doi.org/10.1080/23744235.2020.1806353.
[44] B. Tang, X. Wang, Q. Li, N.L. Bragazzi, S. Tang, Y. Xiao, J. Wu, Estimation of the transmission risk of the 2019-nCoV and its implication for public health interventions, J. Clin. Med. 9 (2) (2020) 462, http://dx.doi.org/10.3390/jcm9020462.
[45] R. Taylor, Interpretation of the correlation coefficient: A basic review, J. Diagn. Med. Sonogr. 6 (1) (1990) 35–39, http://dx.doi.org/10.1177/875647939000600106.
[46] TB health topic WHO, 2021, [Online; accessed 2021]. URL: https://www.who.int/health-topics/tuberculosis.
[47] TB medical review, 2021, URL: https://www.medicinenet.com/is_tuberculosis_tb_contagious/article.htm.
[48] P.K. Tiwari, R.K. Rai, S. Khajanchi, R.K. Gupta, A.K. Misra, Dynamics of coronavirus pandemic: effects of community awareness and global information campaigns, Eur. Phys. J. Plus 136 (10) (2021) http://dx.doi.org/10.1140/epjp/s13360-021-01997-6.
[49] P. van den Driessche, J. Watmough, Reproduction numbers and sub-threshold endemic equilibria for compartmental models of disease transmission, Math. Biosci. 180 (1–2) (2002) 29–48, http://dx.doi.org/10.1016/s0025-5564(02)00108-6.
[50] H. Waaler, A. Geser, S. Andersen, The use of mathematical models in the study of the epidemiology of tuberculosis, Am. J. Public Health Nations Health 52 (6) (1962) 1002–1013, http://dx.doi.org/10.2105/ajph.52.6.1002.
[51] H.T. Waaler, M.A. Piot, Use of an epidemiological model for estimating the effectiveness of tuberculosis control measures. Sensitivity of the effectiveness of tuberculosis control measures to the social time preference, Bull. World Health Organ. (ISSN: 0042-9686) 43 (1970) 1–16.
[52] WHO, Impact of the COVID-19 Pandemic on TB Detection and Mortality in 2020, Tech. rep., World Health Oganization, 2021, URL: https://www.who.int/publications/m/item/impact-of-the-covid-19-pandemic-on-tb-detection-and-mortality-in-2020.
[53] J. Zhang, Y. Li, X. Zhang, Mathematical modeling of tuberculosis data of China, J. Theoret. Biol. 365 (2015) 159–163, http://dx.doi.org/10.1016/j.jtbi.2014.10.019.
[54] F. Zhou, T. Yu, R. Du, G. Fan, Y. Liu, Z. Liu, J. Xiang, Y. Wang, B. Song, X. Gu, L. Guan, Y. Wei, H. Li, X. Wu, J. Xu, S. Tu, Y. Zhang, H. Chen, B. Cao, Clinical course and risk factors for mortality of adult inpatients with COVID-19 in Wuhan, China: a retrospective cohort study, Lancet 395 (10229) (2020) 1054–1062, http://dx.doi.org/10.1016/s0140-6736(20)30566-3.
[55] N. Zhu, D. Zhang, W. Wang, X. Li, B. Yang, J. Song, X. Zhao, B. Huang, W. Shi, R. Lu, P. Niu, F. Zhan, X. Ma, D. Wang, W. Xu, G. Wu, G.F. Gao, W. Tan, A novel coronavirus from patients with pneumonia in China, 2019, N. Engl. J. Med. 382 (8) (2020) 727–733, http://dx.doi.org/10.1056/nejmoa2001017.